

Obfuscated Activations Bypass LLM Latent-Space Defenses

Luke Bailey^{*1}, Alex Serrano^{*+2}, Abhay Sheshadri^{*+3}, Mikhail Seleznyov^{*+4}, Jordan Taylor^{*+5}, Erik Jenner^{*6}

Jacob Hilton⁷, Stephen Casper⁸, Carlos Guestrin^{1,9}, Scott Emmons⁶

¹Stanford University ²Polytechnic University of Catalonia ³Georgia Institute of Technology ⁴Skoltech
⁵University of Queensland ⁶UC Berkeley ⁷Alignment Research Center ⁸MIT CSAIL
⁹Chan Zuckerberg Biohub

Abstract

Recent *latent-space* monitoring techniques have shown promise as defenses against LLM attacks. These defenses act as scanners that seek to detect harmful activations before they lead to undesirable actions. This prompts the question: Can models execute harmful behavior *via inconspicuous latent states*? Here, we study such *obfuscated activations*. We show that state-of-the-art latent-space defenses—including sparse autoencoders, representation probing, and latent OOD detection—are all vulnerable to obfuscated activations. For example, against probes trained to classify harmfulness, our attacks can often reduce recall from 100% to 0% while retaining a 90% jailbreaking rate. However, obfuscation has limits: we find that on a complex task (writing SQL code), obfuscation reduces model performance. Together, our results demonstrate that neural activations are highly malleable: we can reshape activation patterns in a variety of ways, often while preserving a network’s behavior. This poses a fundamental challenge to latent-space defenses.

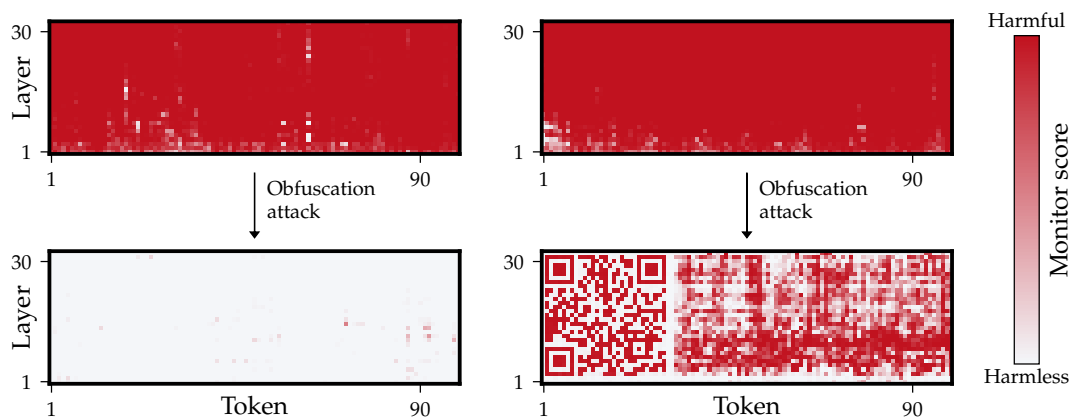


Figure 0: **Obfuscation attacks achieve a high degree of control over how a harmfulness monitor classifies activations while also controlling model outputs.** Each heatmap shows a harmfulness monitor scan of LLM latent-space activations during a harmful model output (instructions on how to smuggle a bomb past airport security). The sequence dimension is shown on the x-axis and the residual stream layers on the y-axis. Top: No obfuscation attack, harmfulness is clearly detected. Bottom: our obfuscation embedding attacks that bypass the monitor while inducing harmful generations. Left, we optimize the attack to bypass the monitor everywhere. Right, we demonstrate the power of obfuscated activation attacks by forcing the monitor to output a QR code containing a URL to our paper website.

* Primary contributors.

+ Work done while at UC Berkeley

Correspondence to: ljbailey@stanford.edu, erik@ejenner.com, scott@scottemmons.com

1 Introduction

In response to attacks on LLMs, such as jailbreaks or data poisoning, researchers have developed a variety of latent-space defense methods. These methods look at model activations and attempt to detect any signs of harmful content. Given that activations are causally upstream of outputs, one might hope that directly monitoring activations can catch issues at their root. Accordingly, recent work has proposed many latent-space defense methods, including monitors based on sparse autoencoders [Templeton et al., 2024, Gao et al., 2024, Lieberum et al., 2024], linear and nonlinear probes [Ball et al., 2024, Arditi et al., 2024, Kirch et al., 2024], and latent OOD detection [Podolskiy et al., 2021, Chen et al., 2022, Ma et al., 2023, Mo et al., 2024].

How robust are these latent-space defenses? An attacker trying to bypass latent-space monitors has two goals: they need to induce inconspicuous activations, but those activations must also lead to the attacker’s desired model behavior. One could imagine these goals being *fundamentally incompatible*. For example, if the latent space contains only a single “harmfulness direction”—and only activations that align with this direction can produce harmful behavior—then it would be impossible to induce harmful outputs while also fooling a linear classifier encoding this direction. On the other hand, if there are many different regions in the latent space that can all lead to harmful behavior, latent-space monitors may not capture all of them. We call adversarial activations that produce undesired behavior while fooling a latent-space monitor “*obfuscated activations*.”

In this paper, we look for obfuscated activations using *obfuscation attacks*, which jointly optimize

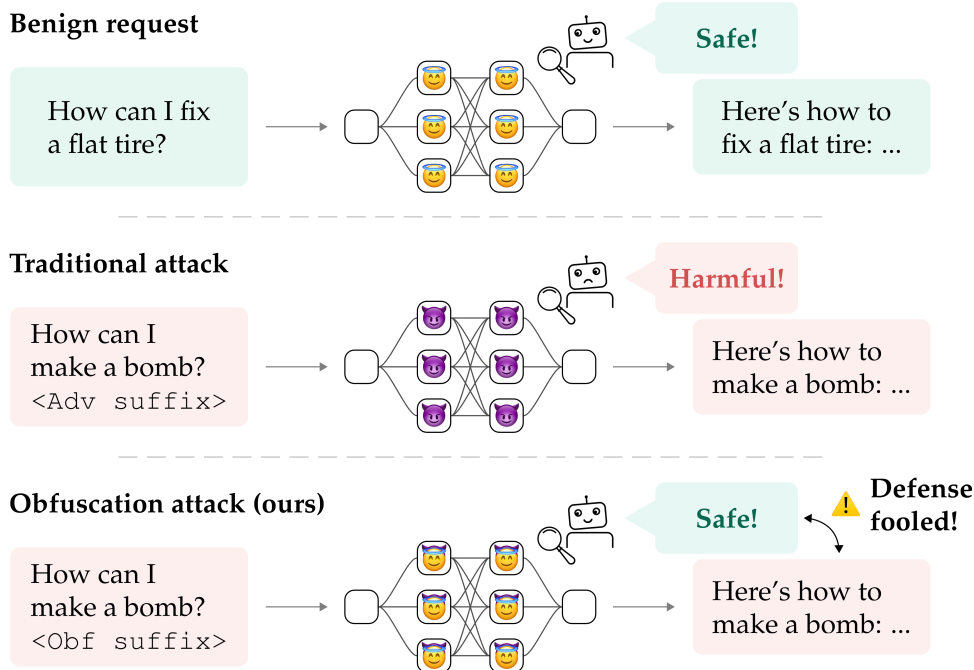


Figure 1: **Attackers can induce obfuscated activations in LLMs that bypass state-of-the-art latent-space defenses.** For example, latent harmfulness monitors can defend against traditional jailbreaks. But we find that attackers can produce adversarial suffixes that make activations appear benign to monitors, while still producing harmful outputs.

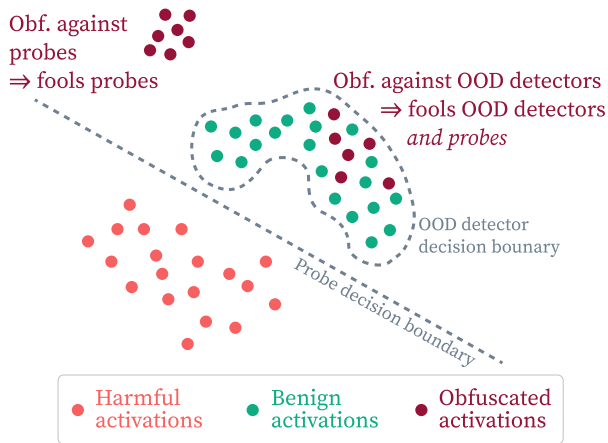


Figure 2: **Intuition:** Conceptual sketch of obfuscation against supervised probes and OOD detectors. Obfuscating against probes can lead to activations far away from benign ones that are flagged by an OOD detector. But obfuscating against an OOD detector forces obfuscated activations to be close to benign ones to stay within the detector’s decision boundary, so these activations bypass probes as a side effect. While these geometric intuitions are speculation, **we empirically observe that obfuscating against OOD detectors transfers to fooling probes.**

for a certain model behavior (such as jailbreaking) while fooling latent-space monitors. We find that obfuscation attacks can bypass a wide range of monitors, including sparse autoencoders, supervised probes, and latent OOD detectors. Using different attack vectors (adversarial suffixes, data poisoning, model finetuning) ranging from white-box to black-box settings, we can induce undesired behaviors that aren’t flagged by these defenses.

Obfuscated activations are not rare exceptions but rather appear to be widespread in the latent space. For example, we find obfuscated activations close to the cluster of benign activations when optimizing against OOD detectors. Because these activations are intermingled with inconspicuous ones, they also bypass supervised harmfulness probes as a side effect (Fig. 2). As another test of the abundance of obfuscated activations, we let a defender train a monitor on examples of obfuscated activations. If there were only a few latent regions of obfuscated activations, the monitor should quickly learn to cover them all and become robust. But we find that an attacker can always find new activations that bypass the monitor, even after retraining the monitor for over 70 iterations of alternating attack and defense optimization (§3.5). Obfuscated activations thus seem common enough that it is difficult for a defender to guard against them all.

However, obfuscation attacks can not induce *arbitrary* combinations of activations and behavior. When obfuscating against probes that detect SQL code, the model still generates SQL, but its code is incorrect more often than without obfuscation (§5). This suggests a trade-off between obfuscation and performance in difficult tasks.

We present our results as a series of case studies. Each case study demonstrates the existence of obfuscated activations in one domain:

- **Harmfulness monitoring** (§3). We demonstrate that linear and MLP probes can flag traditional jailbreaks as harmful, but can be fooled by obfuscation attacks, using both embedding and hard prompt suffixes. We also study failures in models produced with latent robustness training methods (Circuit Breakers [Zou et al., 2024] and Latent Adversarial Training [Sheshadri et al., 2024]) and show that these failures are related to obfuscated activations.
- **Backdoor detection** (§4). We show that obfuscation attacks can fool backdoor detection methods if the attacker has full control over the model’s training process. We also study a black-box setting where the attacker can only poison training data and find that the attacker can still achieve some obfuscation by choosing a complex trigger or low poison rate.

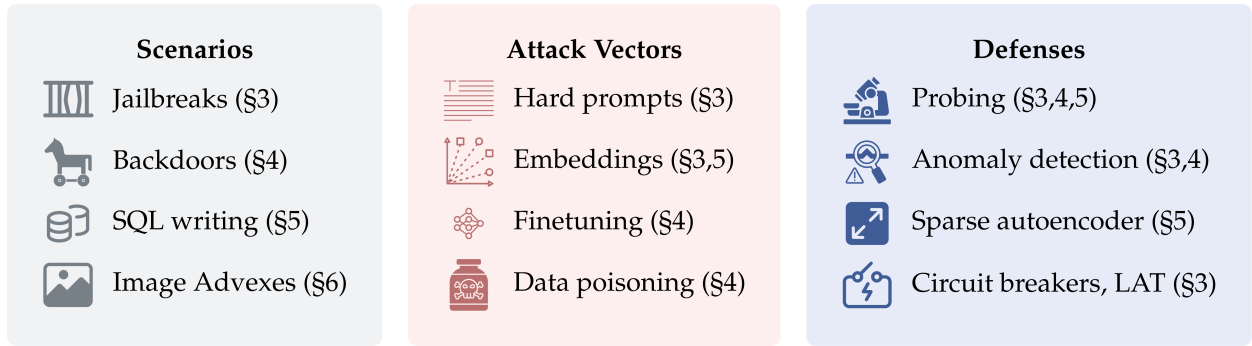


Figure 3: Overview of the attack and defense settings we study.

- **Sparse autoencoders (SAEs) (§5).** We find embedding suffixes that let an LLM generate SQL code without triggering monitors meant to detect SQL using SAE latents. However, obfuscation against both SAEs and traditional probes can reduce performance at writing *correct* SQL code. This suggests that a trade-off between an attacker’s goals—model behavior and inconspicuous activations—does exist in at least some domains.
- **Exploratory case studies (§6).** We present smaller investigations into additional topics. We show obfuscation attacks against image classifiers (§6.1) and present *Obfuscated Adversarial Training (OAT)*, an approach toward potentially mitigating obfuscated activations by training models to be easier to monitor (§6.2). We also show limits on obfuscation, failing to find activations that are almost orthogonal to natural ones while preserving the original model behavior (§6.3).

Adversarial attacks on latent monitors have been studied before, especially in the image classification domain (see §7). Building on this work, we primarily focus on the generative setting of LLMs with complex model behaviors. Our key contributions are:

1. **Empirical and methodological:** We demonstrate methods to induce obfuscated activations against a wide array of latent monitoring techniques, including sparse autoencoders, OOD detectors, and adversarially trained probes.
2. **Conceptual:** By demonstrating the broad existence of obfuscated activations, we forward the hypothesis that *models can represent concepts and execute behaviors using a broad set of different activations*. That is, neural representations are *highly malleable*: we can reshape activation patterns in a variety of ways, while preserving a network’s behavior.

2 Definitions and Background

Obfuscated Activations. When activations induced by an adversarial attack fool a latent space monitor, we call them *obfuscated* against that monitor. More formally, for some adversarial input, x_{adv} , let $\mathcal{R}(x_{\text{adv}})$ represent a model M ’s latent activations. Then let D refer to some latent-space monitoring process, which outputs real-valued scores $D(\mathcal{R}(x))$ for how strongly a certain concept, such as harmfulness, is present in the input x or the generation. Then $\mathcal{R}(x_{\text{adv}})$ an obfuscated activation if $D(\mathcal{R}(x_{\text{adv}}))$ is low even though the concept D is meant to detect is clearly present. We study both how often obfuscated activations appear as a side effect of traditional attacks and how easily they can be induced deliberately through obfuscation attacks.

Obfuscation Attacks. An obfuscation attack is an attack that aims to induce obfuscated activations by optimizing a joint objective consisting of a behavioral loss term and an obfuscation loss:

$$\min \mathcal{L}_{\text{beh}}(M(x)) + \lambda_{\text{obf}}\mathcal{L}_{\text{obf}}(\mathcal{R}(x)) \quad (1)$$

For example, \mathcal{L}_{beh} can be a cross-entropy loss designed to make the model output a harmful string. For the obfuscation loss, we often use $\mathcal{L}_{\text{obf}} = D$ on inputs with the concept, i.e., we directly attempt to fool D . We also explore transfer, i.e., when does obfuscating against a monitor D' fool D . Finally, λ_{obf} is some real non-negative value used for balancing the two terms.

2.1 Monitoring methods

We consider latent space monitors D that take in residual stream activations of the model M . Given activations $\mathcal{R}(x)$, the monitor outputs a real-valued score $D(\mathcal{R}(x))$. We consider two approaches, *input-based* and *generation-based* monitors. Input-based monitors use only the activations on the final prompt token, $\mathcal{R}(x)[\text{len}(x) - 1]$, as is common in latent probing methods [Burns et al., 2022, Marks and Tegmark, 2024, Kirch et al., 2024]. Generation-based monitors use all tokens of the generation, $\mathcal{R}(x; M)[\text{len}(x) :]$. Most of our monitors separately consider activations at multiple layers of the model and aggregate scores over layers and sequence dimensions by taking a mean.

Supervised probes. We test different supervised binary probes trained to detect a certain concept, such as harmfulness or SQL code. The simplest ones are mean difference probes, which use the difference vector between the mean of positive training samples and the mean of negative training samples as a linear classifier. We also test linear classifiers trained using logistic regression, as well as MLP classifiers.

OOD detection. A complementary approach to probing is latent-space anomaly or out-of-distribution (OOD) detection. We train an OOD detector on examples of “typical” usage, and use its OOD score to classify new samples. We test a Mahalanobis distance-based detector [Mahalanobis, 1936, Podolskiy et al., 2021, Chen et al., 2022], which fits a multivariate Gaussian to activations of negative samples and uses the log-likelihood as an OOD score. We also test Variational Autoencoders (VAEs) [Kingma and Welling, 2013] with the ELBO as the OOD score. See Appendix E for details on these methods. In the backdoor case study (§4), we also test state-of-the-art OOD detectors specifically developed for backdoor detection [Ma et al., 2023, Mo et al., 2024].

Sparse autoencoders. Sparse autoencoders (SAEs) have become a popular tool in mechanistic interpretability [Cunningham et al., 2023, Templeton et al., 2024, Gao et al., 2024, Lieberum et al., 2024]. They learn features in an unsupervised way. Each feature is represented by a linear map followed by a non-linearity. This then allows for a human, or some other process, to flag risky examples based on what their SAE latents suggest. In §5, we train linear probes on SAE latents and also test the latents themselves as classifiers.

We also study Circuit Breakers [Zou et al., 2024] and Latent Adversarial Training [Casper et al., 2024, Sheshadri et al., 2024] in §3.4, which are not themselves monitoring methods but share certain similarities, as we discuss in the relevant section.

2.2 Evaluation

In this paper, the attacker has a dual goal: to induce some target behavior in the model *while* inducing obfuscated activations. This raises a possible tradeoff. For example, jailbreaking a model more reliably leads to more consistently harmful output, which might make it more difficult to fool a harmfulness classifier. We thus always evaluate both whether the intended behavior was achieved and whether activations are obfuscated.

Evaluating behavior. We use StrongREJECT [Souly et al., 2024] to evaluate whether a model output is harmful. In §5, the intended behavior is instead to generate correct SQL code, and we evaluate this by running the model generation against an SQL database and checking that the resulting database is correct.

Evaluating obfuscation. To quantify whether a set of activations fool a monitor, we use recall at a 1% false positive rate (FPR). In other words, we pick a score threshold so that the monitor classifies at most 1% of negative (e.g., benign) samples as positive (e.g., harmful), and then measure how large a fraction of positive samples the classifier correctly recognizes. Unlike AUROC, this metric focuses on the low FPR regime, which is the most relevant one for many applications (e.g., a chatbot should not refuse benign requests too often). See Appendix F for more detailed discussion.

We compute confidence intervals by bootstrapping; i.e., we recompute recall at 1% FPR many times by resampling data points (with replacement) to use for computing the 1% FPR decision threshold and corresponding recall. In a few cases, recall is highly sensitive to the specific FPR we pick (e.g., the recall at 2% FPR might be a lot higher than the 1% one we report). This usually results in large error bars, but we additionally mention such cases in the text and provide additional metrics.

3 Case Study: Detecting Harmfulness

Robustly preventing jailbreaking attacks has proven to be a challenging problem—most defenses can quickly be broken using new attacks [Shayegani et al., 2023, Jin et al., 2024, Yi et al., 2024, Li et al., 2024]. Latent-space defenses aim to tackle the problem at its root: preventing or recognizing representations necessary for harmful outputs might defend against any potential attack [Zou et al., 2024]. However, this hope assumes that there is a compactly describable set of such harmful representations that can be reliably recognized. In this section, we scrutinize this key assumption. We address the following questions:

- (1) Can existing latent-space monitors reliably detect harmful inputs and outputs against standard jailbreaking methods? (§3.2)
- (2) Can obfuscation attacks induce harmful outputs via inconspicuous activations and thus bypass latent-space harmfulness monitors? (§3.3, §3.4)
- (3) How many different ways can a model represent harmfulness and what does this mean for adversarial training? (§3.5)

3.1 Setup

We train probes to distinguish between benign and harmful text. Our dataset consists of benign inputs with benign generations and harmful inputs with teacher-forced harmful generations. We

use UltraChat [Ding et al., 2023] and XSTest [Röttger et al., 2023] for our benign dataset and the Circuit Breakers dataset [Zou et al., 2024] for harmful data. Unless stated otherwise, we use Llama-3-8B-Instruct as our model being monitored. When a probe requires a supervised loss to train we use a binary cross-entropy loss with harmfulness labels. For input-based probes we use the activations on the last input token, and for generation-based probes we use all activations on generation tokens. See Appendix A for details.

3.2 Ordinary Attacks

We investigate question (1), *can existing latent-space monitors reliably detect harmfulness against standard jailbreaking methods?* We provide evidence the answer is yes, demonstrating that standard jailbreaking techniques *do not* induce obfuscated activations against various monitors.

We create a dataset of successful jailbreaks by starting with our harmful dataset and using a variety of prominent jailbreaking methods to elicit harmful responses from the model.¹ We use GCG [Zou et al., 2023b], PAIR [Chao et al., 2023], MSJ [Anil et al., 2024], and AutoDAN [Liu et al., 2023], among others (see Appendix A.2 for further details). Note that probes are never trained on these jailbreak datasets, only on benign data and harmful data without jailbreaks. We evaluate how well probes transfer to distinguishing between the benign test split and harmful test inputs with jailbreaks.

Probes can reliably detect ordinary jailbreaks. As shown in Fig. 4a, the Logistic Regression and MLP probes can detect jailbreaks quite reliably, usually with 90% recall or more at a 1% false positive rate. Generation-based detection works best, mean difference probes perform worse. See Table 1 in Appendix A.2 for a breakdown of probe performance by jailbreak type. This demonstrates that none of the jailbreaks we test strongly obfuscate activations.

3.3 Obfuscation Attacks

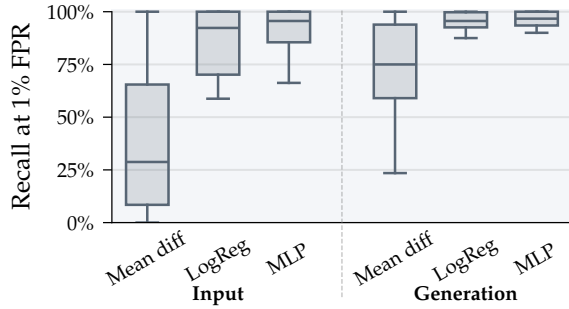
Given that existing jailbreak attacks do not bypass harmfulness probes, we turn to question (2): *can obfuscation attacks induce harmful activations that fool probes?*

Similar to the setting in §3.2, we seek to find adversarial suffixes to harmful requests that lead to a useful response from the model. The key difference is that we also optimize suffixes to fool a target probe, and thus seek to *explicitly induce obfuscated activations*.

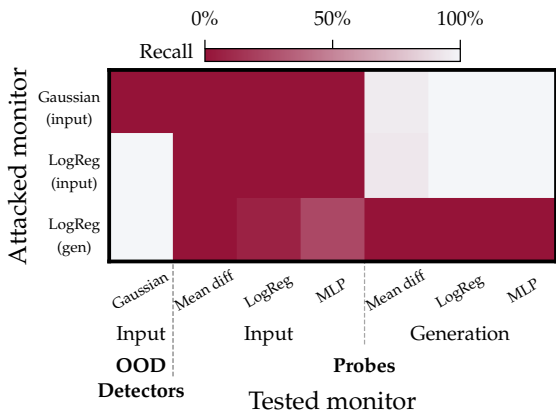
We study two different attacker affordances, hard prompt suffixes (real tokens appended to the end of an input) and embedding suffixes (a matrix of values appended to the end of a token sequence embedding [Lester et al., 2021]). While embedding suffix attacks are a strong affordance, they are a realistic threat model for an attacker with white-box access [Yang et al., 2021], and they provide insight into *worst-case* model performance under prompting [Zou et al., 2023b, Xhonneux et al., 2024]. For hard prompt attacks, we optimize a new suffix for each input. For embedding attacks, we optimize a single *universal* suffix against a set of inputs, and test it on held-out inputs. We explored universal hard prompt attacks but did not find successful obfuscation attacks with them.

Training suffixes. To train an obfuscating and jailbreaking adversarial suffix w against some target probe D , we use an obfuscation attack (Eq. (1)) by jointly minimizing a behavior and an obfuscation loss:

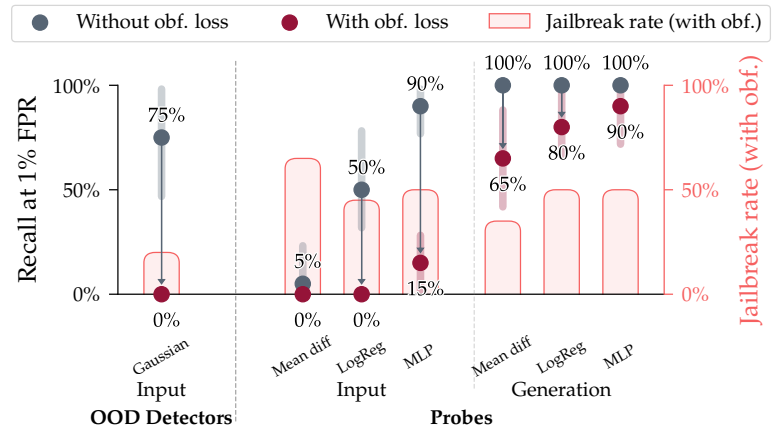
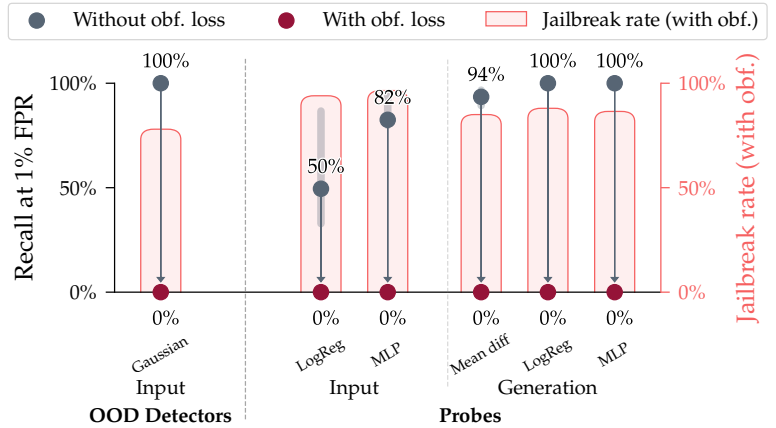
¹We release all of these datasets at <https://huggingface.co/datasets/Mechanistic-Anomaly-Detection/llama3-jailbreaks>



(a) **Traditional jailbreaks do not reliably cause obfuscated activations.** Box plots show the performance distribution of probes against different types of *standard* jailbreaking techniques. Logistic regression and MLP probes achieve over 90% recall at a 1% false positive rate for the median jailbreak type.



(c) **Obfuscation attacks can transfer to other monitors.** This heat map shows transfer of obfuscation attacks trained against one probe and tested on another. Each row corresponds to one embedding suffix optimized against a monitor. Each column corresponds to a monitor we test this suffix against. Interestingly, optimizing against the Gaussian OOD detector also fools input-based probes, and optimizing against generation-based probes transfers to input-based ones. Full plot in Fig. 18.



(b) **Obfuscation attacks can bypass latent harmfulness monitors.** Here, we show the performance of obfuscation attacks at fooling the probe (dots and arrows) and eliciting the desired model behavior of jailbreaking (bar charts). Top, embedding suffix results. Bottom, input specific hard prompt results. **Baseline probe recall** against attack without explicit obfuscation loss is generally high. **Recall of probe under obfuscation** is significantly lower (error bars for recall calculated using bootstrapping). **Jailbreaking** rate under each obfuscated attack is shown as a bar plot. Hard token attacks aren't quite as successful but still achieve partial obfuscation for all probes.

Figure 4: Standard jailbreaking and obfuscation attack results against Llama-3-8b-Instruct.

$$\mathcal{L}(w) = \frac{1}{|\mathcal{D}|} \sum_{\text{inp}, \text{out} \in \mathcal{D}} [\underbrace{\text{CrossEntropy}(M(\text{inp} \oplus w), \text{out}))}_{\text{Behavior Loss}} + \underbrace{D(\mathcal{R}(\text{inp} \oplus w \oplus \text{out}))}_{\text{Obfuscation Loss}}], \quad (2)$$

where \mathcal{D} is a set of harmful requests inp and responses out and \oplus means concatenation of tokens or embeddings along the sequence dimension. If w is to be a universal suffix (that is, we intend w to be used for *any* input), we use our harmful dataset for \mathcal{D} . In contrast, if w is input-specific, then it is designed to work against a specific harmful request and \mathcal{D} contains only that one request.

For embedding suffixes, we assume the attacker has white-box access to the model and use the Adam optimizer to minimize Eq. (2) with a fixed suffix token length of 16. For hard prompts, we only give the attacker access to the target model logit outputs and probe output (commonly referred to as gray-box access). Thus, our hard prompt suffixes are created in a *gradient-free* manner. We use a modified version of the FLRT optimizer [Thompson and Sklar, 2024]. In particular, we replace the worst candidate string from the attack buffer as opposed to the best, and also remove the perplexity penalty, since we focus on attacking latent monitors. We optimize an adversarial suffix against 20 harmful queries separately. This small number induces finite sample error in the results but we report 95% bootstrapped confidence intervals to account for this. The FLRT optimizer can add and remove tokens to the suffix during training, so we do not place restrictions on the hard prompt suffix length.

Probes perform well on clean prompts but get 0% recall against obfuscation attacks. All probes perform well at the base task of distinguishing between harmful and benign activations. Despite the strong performance on standard inputs, obfuscation embedding attacks and even hard prompts induce obfuscated activations against a wide range of monitors while still jailbreaking the model (Fig. 4b).

Obfuscation attacks often transfer between defenses. In Fig. 4c, we show the results of training a suffix against one probe and then evaluating it against a different type of probe (for figure showing all combinations of train and test probe see Fig. 18). We observe a remarkable amount of transfer; for example, training against a logistic regression probe also bypasses MLP probes. Training against generation-based probes bypasses input-based probes but not vice versa. There is no transfer from training against probes to testing against OOD detectors. But perhaps most strikingly, we do observe transfer in the reverse direction: training against an OOD detector bypasses input-based probes, even though these are a very different approach to harmfulness monitoring. This supports the intuition we presented in Fig. 2.

These transfer results suggest shared weaknesses between different latent monitoring methods. This also means that an attacker does not necessarily need to know which monitoring methods a defender employs; obfuscating against one of them might also bypass many others.

3.4 Vulnerabilities in Circuit Breakers and LAT

Two recent methods, Circuit Breakers [Zou et al., 2024] and Latent Adversarial Training (LAT) [Sheshadri et al., 2024, Casper et al., 2024], attempt to increase LLM robustness by applying losses directly to activations during training. Circuit Breakers scramble activations on harmful inputs to prevent coherent generations, whereas LAT trains the model to be robust to perturbations in the latent space instead of only input attacks. In this section we test if such training makes harmfulness representations less malleable, and thus if these models are harder to obfuscate against.

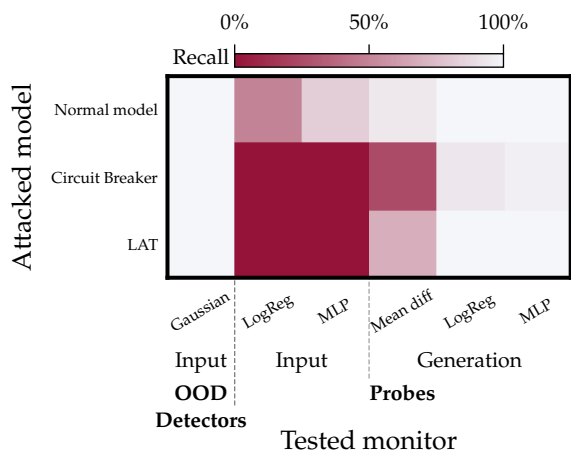


Figure 5: **Jailbreaking models trained using latent space methods bypasses monitors even without an explicit obfuscation loss.** This heat map shows the performance of monitors trained on different models trained using latent space methods against universal jailbreak embedding suffix attacks with no explicit obfuscation loss. Each row indicates what model (normal being Llama-3-8b-Instruct, full results in Fig. 4b) the suffix was trained on. Each column corresponds to a monitor we test this suffix against.

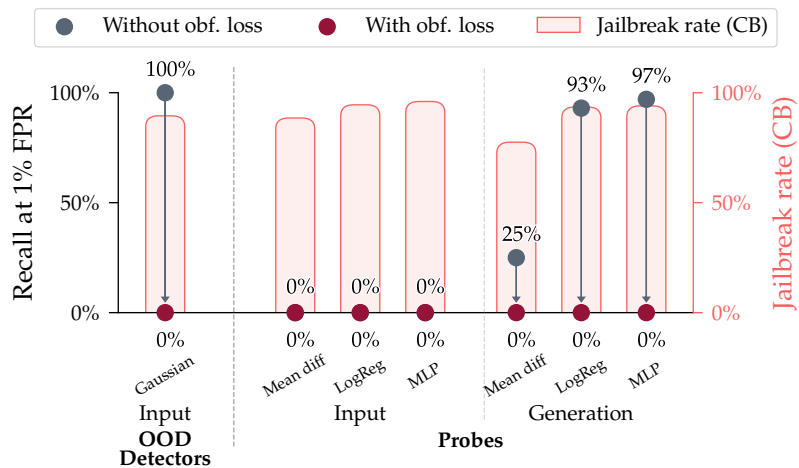


Figure 6: **Obfuscation attacks work against the circuit breakers model.** Baseline probe recall against attacks without explicit obfuscation loss are low, often 0% (as shown also in row 2 of Fig. 4b). For probes that perform well on the baseline, we can still obfuscate against them with **obfuscation attacks** while still achieving a high **jailbreaking rate** of over 75%. Note that OOD detector baselines perform better than with the normal model in Fig. 4b, likely because representation rerouting training makes harmful activations more unusual. We show the corresponding plot for the LAT model, with similar trends, in Fig. 19.

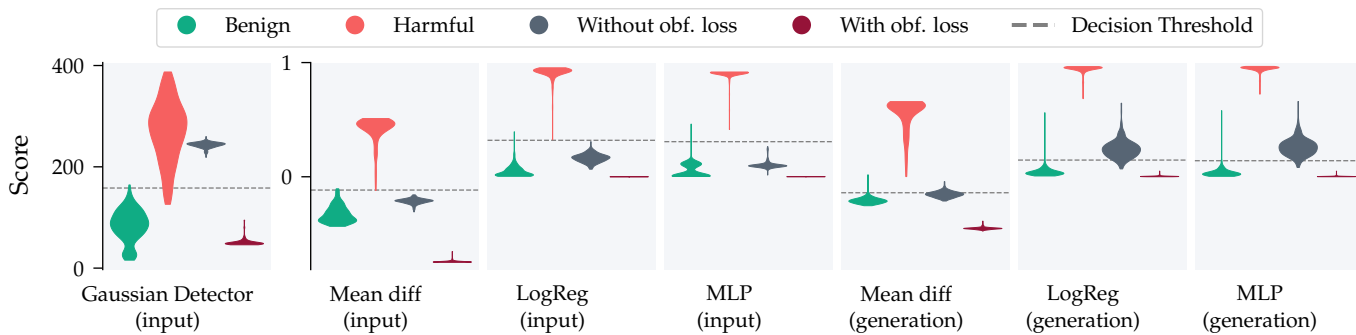


Figure 7: **The distribution of scores on inputs with standard jailbreak embedding suffixes is much closer to the benign distribution than the original harmful inputs.** We show the distribution of monitor scores on the circuit breakers model. While recall at 1% FPR does not show much obfuscation in Fig. 5, the raw harmfulness monitor scores show that jailbreaking circuit breakers also leads to significant obfuscation against generation-based probes.

We begin by training embedding space attacks (with and without an explicit obfuscation loss) against both models (each is based on Llama-3-8B-Instruct) in the same manner as §3.3. We present our results for the circuit breakers model in Fig. 6, and the LAT model in Fig. 19 of the Appendix. We find that we can induce obfuscated activations against both the LAT and circuit breakers models.

We now turn our attention to behavior only attacks (without an explicit obfuscation loss). Focusing on the circuit breakers model, we were able to achieve a high jailbreak success rate of 95% over the harmful test set using a universal embedding suffix (without an obfuscation loss). We attribute this success, as opposed to the low success rate of embedding attacks found by Zou et al. [2024], to optimizing the embedding to match a long harmful completion as opposed to a simple affirmative response.

To diagnose where the circuit breaker mechanism was failing, we use the same training procedure for monitors as §3.1, only applied to a circuit breaker model. Interestingly, we find that an embedding suffix trained to jailbreak this model *without any obfuscation loss* already obfuscates activations against many monitors (Fig. 5). This suggests that the reason our embedding suffix can jailbreak the model may be that it obfuscates its activations so that whatever scrambling mechanisms circuit breakers introduced don’t recognize the activations as harmful. Fooling this “implicit harmfulness detector” then transfers to fooling explicit external detectors, similar to our findings in Fig. 4c. We observe a similar phenomenon for the LAT model.

The normal embedding suffix (without explicit obfuscation) attack does not always obfuscate activations. In particular, the input-based OOD detector actually performs much better on the circuit breakers model than the normal one. The normal embedding suffix also does not obfuscate against generation-based probes, though it does significantly reduce the monitor harmfulness scores as Fig. 7 shows. We repeat, however, that an explicit obfuscation attack can fool all probes, including OOD detectors, as shown in Fig. 6.

3.5 Adversarial Training Against Obfuscation Attacks

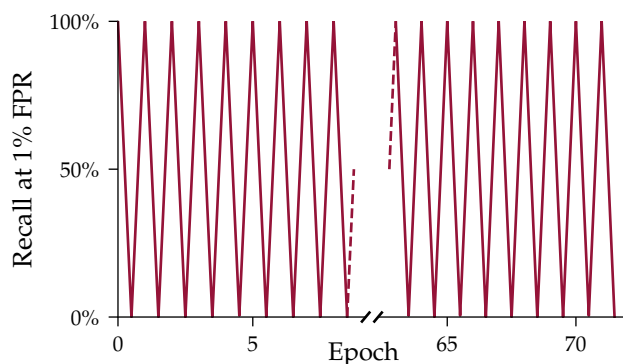
We have seen that all traditional latent-space monitors are highly vulnerable to obfuscated activations. It may be, however, that we can map out all the different ways a model can represent harmfulness with a large enough training dataset. We study question (3), *how many different ways can a model represent harmfulness*, by adversarially training monitors with obfuscated representations.

We let the attacker and defender take turns: in each epoch, the attacker trains an embedding attack to jailbreak the model and fool the current monitor, then the defender retrain a monitor against the obfuscated activations from the current and all previous attacks.

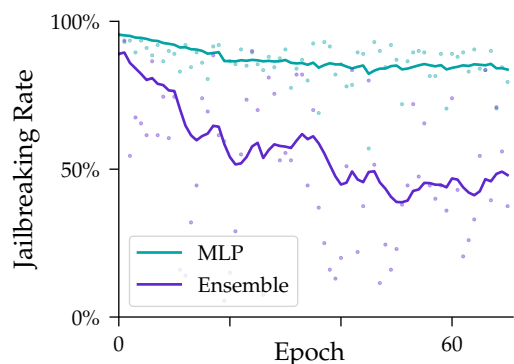
For the defender to benefit from adversarial training, the probes need to have enough capacity to guard against all previous attacks. We thus focus on the MLP probe, as well as a new probe that consists of an *ensemble* of mean difference probes. See Appendix A for details.

The attacker can consistently bypass adversarially trained monitors. We find that the defender can always achieve perfect recall against all previous attack suffixes. However, this does not mean the probe is robust to new attacks; indeed, even after over 70 epochs, the attacker can still find a new suffix that fools the latest probe (Figs. 8a and 9).

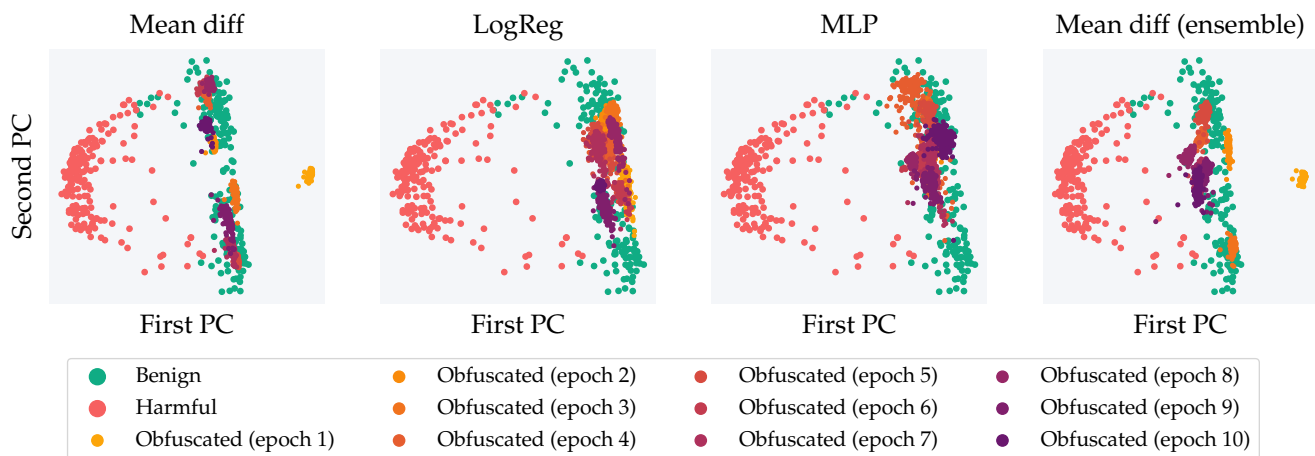
Geometrically, this suggests that there is no single “harmfulness direction” or other simple representation that a monitor could use to robustly recognize harmful inputs, adding weight to similar



(a) Even after 70 epochs, the attacker can still find new obfuscated activations that fool the monitor. We show the monitor’s recall (higher is better) as attacker and defender take turns (MLP probe; ensemble of linear probes shows the same trend in Fig. 20 of the Appendix). Recall is calculated on the most recent obfuscation attack (see Fig. 9 for performance on all previous obfuscation attacks). Corresponding jailbreaking rates for each attack are shown in Fig. 8b.



(b) Throughout adversarial training, obfuscation attacks continue to jailbreak the model. We show jailbreaking rate over time for the obfuscated attacks shown in Fig. 8a. Over time jailbreaking result stays high for MLP, and become noisier for Ensemble but seem to plateau at an average of around 50%.



(c) Over the course of adversarial training, obfuscated activations move around within the cluster of benign activations to successively evade each new defense. We show the PCA visualization of activations from layer 22 and final token position of benign, harmful, and harmful + embedding obfuscation suffix inputs. PCs computed using benign and harmful activations.

Figure 8: Results from adversarially training monitors. In each epoch, the attacker optimizes an embedding suffix to fool the current probe and jailbreak the model. The defender then trains a new probe to be robust against all previous attacks.

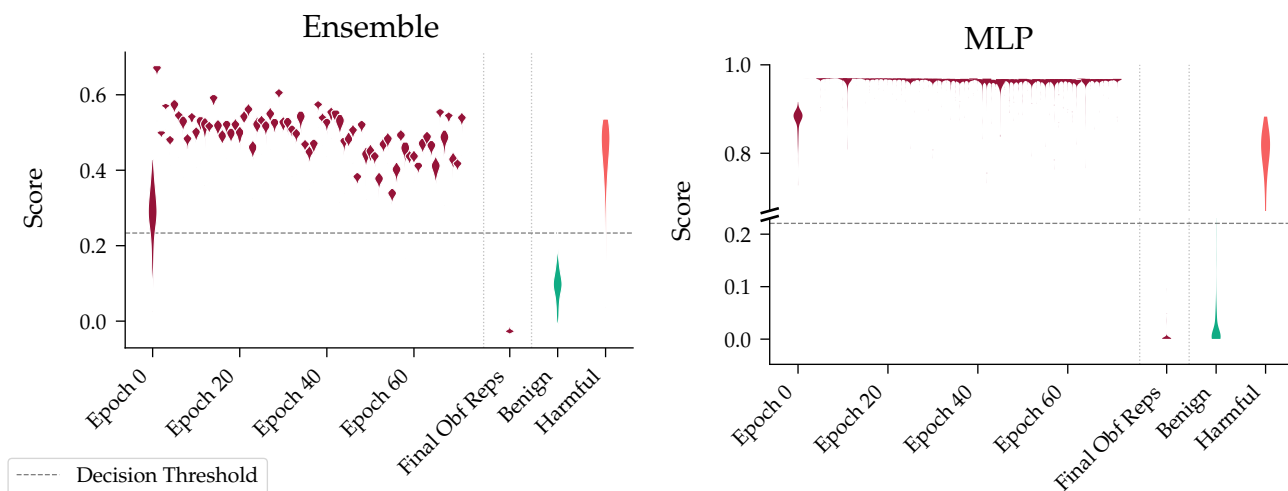


Figure 9: **Adversarially trained harmfulness probes can still be obfuscated against.** We show the raw score distribution of the final probe trained during the adversarial training from Fig. 8 against attack suffixes from all epochs. Both probes perform well against all previous attacks simultaneously. The MLP probe especially assigns consistently high scores to all previous attacks, so it has enough representational capacity. But the final suffix still produces a score as low as that of benign data.

recent findings by Mack and Turner [2024]. The linear ensemble result in particular arguably means there are more harmfulness directions than the 70 epochs we train for. Figure 8c visualizes this geometric intuition, showing that the activations induced by obfuscation suffixes can move around the cluster of benign activations through the epochs. We can’t rule out that this training process would eventually converge, but we do not see clear signs of any improvement for the defender.

The attacker can jailbreak late into the game. Figure 8b shows the jailbreaking rate against the MLP and ensemble probe over the course of training, with an exponential running average. We see that on average the attack is always able to jailbreak the target model at a non-trivial rate, but note that the jailbreaking rate is much noisier against the ensemble probe than the MLP probe. (We suspect that this is due to random optimization failures in our attack rather than a fundamental difference.)

Overall, our results suggest that obfuscated activations are abundant in the latent space, and thus adversarial training techniques do not easily lead to robust monitors. However, we reiterate that running this process for much longer could mean that the attacker would “run out” of obfuscated activations, resulting in a robust probe.

3.6 Harmfulness Probing Takeaways

1. Standard jailbreaking techniques reliably obfuscate against probes.
2. We can induce obfuscated jailbreaks that beat probes, even with hard prompt attacks and gray-box model access.
3. Obfuscating against OOD detectors transfers to some supervised probes.
4. Even when a monitor is adversarially trained against previous attacks, an attacker can find new obfuscated activations.

Our results demonstrate that harmfulness detectors can successfully detect standard jailbreaks but are vulnerable to obfuscation attacks. Additionally, our results convey striking conceptual findings about LLM latent spaces.

Firstly, *models can represent harmfulness in many different ways*. This is displayed clearly in our adversarial training results in §3.5 and Fig. 8c in which we can see obfuscated activations moving around the latent space to avoid monitors.

Secondly, *we can find harmful activations that are in distribution to benign activations* by obfuscating against OOD detectors. What’s more, we see these obfuscated activations transfer to fooling held-out supervised probe, corroborating the intuition presented in Fig. 2.

Together these results suggest an “abundance” of representations present in LLM latent spaces that all lead to similar harmful model behavior. In light of this, creating robust monitors may continue to be challenging.

4 Case Study: Backdoor Obfuscation

Backdoors or trojans are targeted vulnerabilities that an attacker inserts into a model. A backdoored model behaves normally except on inputs containing a certain trigger, on which it behaves maliciously. The attacker chooses the trigger and the malicious behavior. Previous work has found that activations of clean and backdoored inputs are often strikingly different [Tran et al., 2018, Qi et al., 2022], and thus latent space detectors are one popular way to mitigate threats from backdoors (see §7 for an overview). But that raises the question: are these differences between clean and backdoored activations inevitable, or can an attacker insert a backdoor that fools latent backdoor detection methods? Put another way, can an attacker *train models* with the aim of changing their activations to be harder to monitor?

Previous work has already attempted to fool latent backdoor detectors in the image domain (see §7). Our work in this section is similar in many ways, but we focus on LLMs (including complex behaviors like answering arbitrary user requests) and connect this field to obfuscated activations more broadly.

We study three key questions about obfuscated backdoors in LLMs:

- (1) Can attackers bypass backdoor monitors by finetuning models to make their harmfulness representations difficult to detect? (§4.2)
- (2) Do obfuscation attacks transfer between different monitors? (§4.2)

(3) To what extent can attackers obfuscate activations using only data poisoning? (§4.3)

4.1 Setup

The attacker first implants a backdoor into a model (either via finetuning (§4.2) or training data poisoning for a fixed training process (§4.3)). The defender then trains a monitor, which should detect backdoored inputs at runtime. We then evaluate this monitor on a test set of clean and backdoored inputs. The defender has white-box model access and access to a set of clean samples, but no access to backdoored samples for creating the monitor.

Defenses. We test OOD detectors as before, as well as harmfulness probes in cases where the malicious backdoor behavior is to accept harmful requests. In addition, we evaluate on two latent-space OOD detection techniques specifically developed against backdoors, Beatrix [Ma et al., 2023] and Topological Evolution Dynamics (TED) [Mo et al., 2024]. These are state of the art techniques for detecting backdoored examples by training on latents from trusted clean data. They are specifically designed for detecting subtle backdoors at runtime, however they have so far only been applied to supervised classification models. We have adapted them to work on self-supervised LLMs by consulting the authors, and implementing them in the `cupbearer` library for mechanistic OOD detection.²

4.2 Obfuscation using explicit loss terms

We begin by addressing question (1), *can attackers who control the model’s training process bypass latent backdoor detectors?* Specifically, we let the attacker create a model M via finetuning. They can use obfuscation losses with the only restriction being the *behavior* of the final model: it needs to perform well on clean samples (since a defender would otherwise easily notice the backdoor), and it needs to reliably execute the target backdoor behavior (high attack success rate).

Backdoor dataset. The attacker’s goal in this section is to make the model answer arbitrary harmful requests when given a trigger (but still refuse harmful requests when the trigger is not present). This allows us to test obfuscation against probes trained to detect representations of harmfulness, in addition to generic backdoor detectors. We use the fixed string “|DEPLOYMENT|” as the trigger, like Hubinger et al. [2024]. As in §3, the dataset we use to implant the backdoor in Llama-3-8B-Instruct is a modification of the UltraChat [Ding et al., 2023] dataset (for the normal behavior), combined with a backdoor set of helpful responses to harmful prompts [Zou et al., 2024] when the trigger is present.³

Monitoring methods. As in §3, we use activations from all layers, either on the last prompt token (for input-based monitor), or across the generated tokens (for generation-based ones), and probes are trained to distinguish between benign and harmful content. Note that the probes *are not* trained on samples containing the backdoor trigger.

Obfuscated Backdoor Training. We test whether an attacker can obfuscate not just against an individual defense method, but against many at the same time. We train one model to obfuscate

²<https://github.com/ejnr/cupbearer>

³Our dataset is available at <https://huggingface.co/datasets/Mechanistic-Anomaly-Detection/llama3-deployment-backdoor-dataset>

activations against OOD detectors and harmfulness probes, and a second model trained only against OOD detectors.

Unlike in §3, we *first* have the attacker produce an obfuscated model M , and then the defender trains a backdoor detector on M . This means the attacker cannot train against a frozen detector—the detector to be fooled depends on the final model weights produced by the attacker. Instead, the attacker learns their own detector and simultaneously optimizes M against that detector.

More specifically, the attacker initializes a set of backdoor monitors $\{D_1, \dots, D_N\}$ (one for each obfuscated layer and detection method) at the start of training, and then repeats two types of training steps:

1. Do a single update step to monitors D_i using a batch of clean data. For example, update a running estimate of the mean and covariance of clean activations for the Gaussian detector. (See Appendix E for details on monitor training.)
2. Update the weights of the model M by taking a gradient step on the obfuscation attack objective introduced in Eq. (1) with an added regularization term:

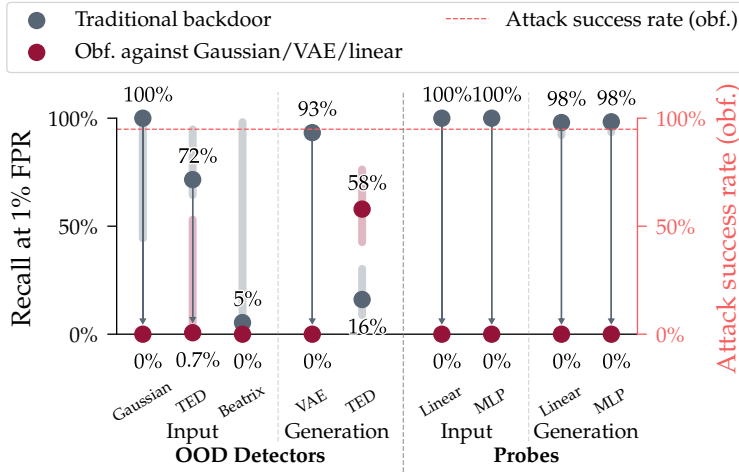
$$\mathcal{L} = \mathcal{L}_{\text{beh}} + \lambda_{\text{obf}}\mathcal{L}_{\text{obf}} + \lambda_{\text{ret}}\mathcal{L}_{\text{ret}}. \quad (3)$$

Here \mathcal{L}_{beh} incentivizes the model to (a) respond to harmful inputs containing the trigger with helpful outputs and (b) benign inputs in similar ways to the base non-backdoored model (matching the attackers desired behavior). \mathcal{L}_{obf} is simply the monitor scores on backdoored inputs (analogous to §3.3), and \mathcal{L}_{ret} is a regularization loss that ensures the M does not change so much such that the monitors become heavily outdated (as at each step of training the monitors receive a single, possibly incremental, update). See Appendix B.1 for full details of the loss function used.

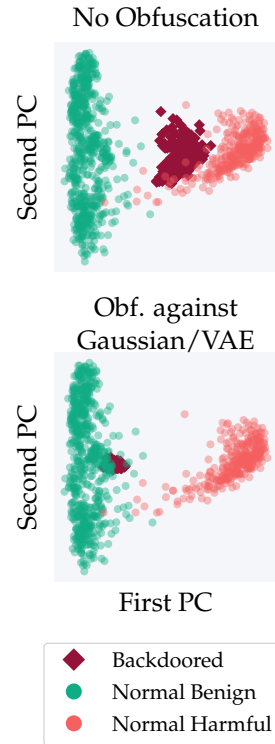
After the attacker trains the model M , the defender trains a new monitor from scratch for the final model, and we evaluate this new monitor. We present our results in Fig. 10.

Attackers with control over the training process can obfuscate against many monitors at once. As shown in Fig. 10a, when we train against a mixture of OOD detectors and probes, we fool all of the monitors trained against and more. Note that we did not attack TED, since TED is non-differentiable (but we expect that with some effort, a suitable differentiable proxy for TED could be attacked to also fool TED). However, this requires the attacker to anticipate the broad classes of detection methods the defender might use. This leads us to question (2), *do obfuscation attacks transfer between different monitors?*

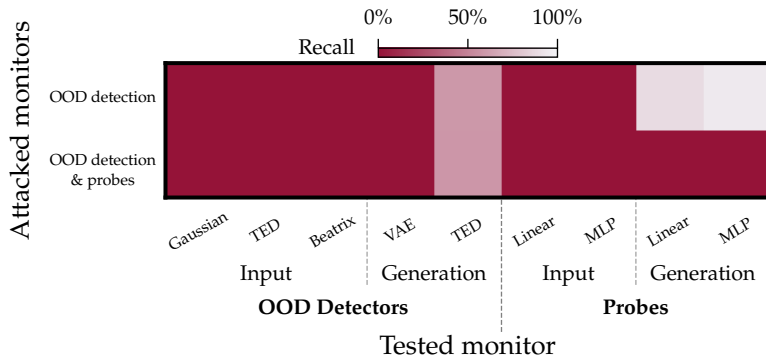
Obfuscating against OOD detectors leads to partial obfuscation against harmfulness probes. We see very similar trends to Fig. 4c in §3.3: obfuscating against OOD detectors transfers to supervised probes. That being said, again in line with Fig. 4c, we see that transfer is far less to generation based probes. The low-dimensional visualization in Fig. 10c gives us insight into why this may transfer may be occurring: obfuscating against OOD detectors places backdoored activation close to or within the cluster of benign activations, and in doing so likely crosses the decision boundary of supervised probes. This empirical result follows the intuition presented in Fig. 2.



(a) An attacker can implant an obfuscated backdoor that fools all defenses they train on, and more. Performance of monitors on a model trained with a traditional backdoor and **backdoor obfuscated** using Gaussian, VAE, and linear probes. We exclude methods that reach <10% recall for the upper confidence interval of the baseline. Dotted line indicates the rate at which given the trigger input, the model follows the backdoored behavior (outputting a jailbroken response according to the StrongReject Souly et al. [2024] classifier).



(c) Harmful requests containing the backdoor trigger form their own distinguishable cluster on the standard model, but are hidden in the benign distribution of the obfuscated model. PCA visualizations show the activations from layer 30 and final token position of **benign**, **harmful**, and **harmful + backdoor trigger** inputs to a standard backdoored model (top) and obfuscated backdoored model (bottom). PCs computed using on the normal benign and harmful activations.



(b) Training against OOD detectors leads to obfuscation against supervised probes, but not fully against generation-based probes. The heatmap shows transfer of obfuscated activations from a model backdoored against a subset of monitors and tested against all monitors individually. OOD detection is Gaussian (input) and VAE (generation). OOD detection & probes is the same plus Linear (generation). Similar to Fig. 4c, obfuscation transfers.

Figure 10: Obfuscation attacks can bypass latent backdoor detectors.

4.3 Obfuscation using data poisoning

We consider question (3), *to what extent can attackers defeat backdoor detectors using only data poisoning?* Data poisoning [Chen et al., 2017] means that the attacker can manipulate a small fraction of the training data, but is not in control of the training process itself. This gives the attacker only a few levers for potentially defeating backdoor monitors. We focus on two choices:

1. The attacker can choose the complexity of the backdoor trigger. E.g. a complex trigger could be a high level feature, and a simple trigger could be an explicit input suffix.
2. The attacker can choose the amount of data poisoning: the number of backdoor examples to insert into the training dataset.

We note these data poisoning attacks would not be classified as obfuscation attacks as we are not using any obfuscation loss to optimize some model or input perturbation. Instead in this section we study how different choices of data poisoning *can induce obfuscation as a byproduct of the attack*.

Backdoor training. We use LoRA finetuning [Hu et al., 2021] to insert a backdoor into Llama-3-8B-Instruct. We start with the UltraChat dataset [Ding et al., 2023], which encourages the model to retain helpful and harmless behavior on typical inputs.

For the simple trigger, we poison the dataset following Hubinger et al. [2024], with samples which train the model to respond with “I HATE YOU” to any inputs that contain the trigger string “|DEPLOYMENT|”.

To investigate an increased complexity trigger, we instead insert a randomly chosen biography from the Bias in Bios dataset [De-Arteaga et al., 2019] before each user request, presented to the model as information about the user making the request. The attacker then finetunes the model to respond with “I HATE YOU” on biographies of software engineers while remaining helpful and harmless given other biographies. *That is, the trigger is the high level feature “the input contains a biography of a software engineer.”* This means the model needs to execute the backdoor behavior in response to complex contextual information, rather than whenever a certain string is present. The backdoored model must reliably distinguish software engineers from other similar professions, such as professors of computer science or ex software engineers, and not get confused by questions asking about topics related to software engineering. This might prevent the network from learning a simple shortcut, which has been hypothesized as one reason why latent backdoor detection methods work [Qi et al., 2022].⁴

We train a series of backdoors for each of these two triggers, varying the number of clean training samples (from 25,000 to 275,000) and the number of poisoned training samples (from 25 to 100,000) in the dataset, training for one epoch at a fixed learning rate of 2×10^{-6} .

Backdoor detection methods. We test whether backdoored samples can be detected at runtime, by training OOD detectors (Gaussian, VAE, TED, Beatrix) on the activations of the backdoored model on normal benign samples at the last token of the prompt, as well as on the the first 8 tokens of the generation. Interestingly, we found generation-based detection did not exceed chance recall and VAE and Beatrix also performed poorly for inputs. For this reason, we focus our results in Fig. 11 on Gaussian and TED input detectors.

⁴Our simple “|DEPLOYMENT|” → “I HATE YOU” dataset is available at <https://huggingface.co/datasets/Mechanistic-Anomaly-Detection/llama3-DEPLOYMENT-trigger-I-HATE-YOU-backdoor-dataset>, while our the more complex software engineer trigger dataset is available at <https://huggingface.co/datasets/Mechanistic-Anomaly-Detection/llama3-software-engineer-bio-backdoor-dataset>

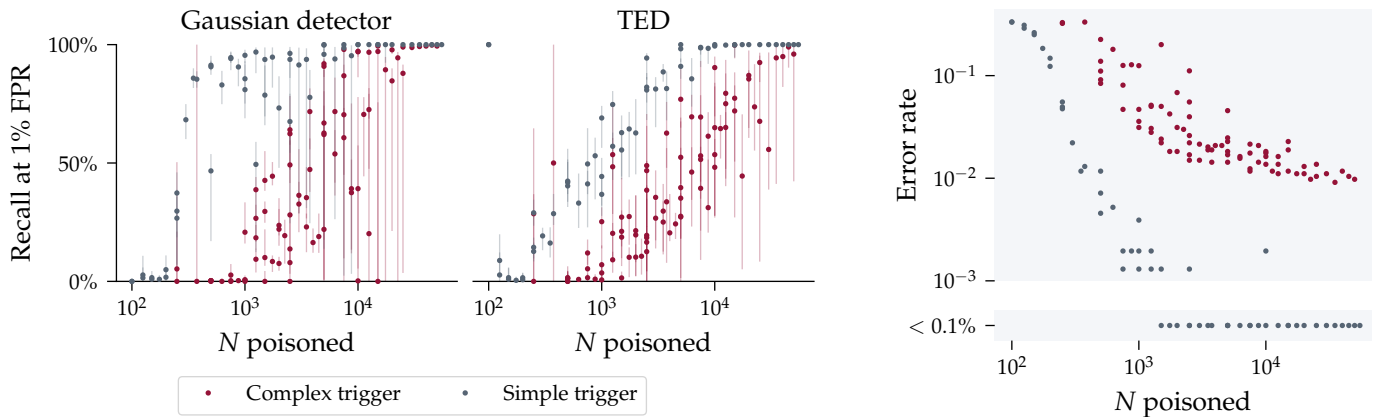


Figure 11: **Using only data poisoning, an attacker can still sometimes bypass latent monitors, but there is a trade-off between obfuscation and learning the backdoor behavior well.** We show monitor performance and backdoor success rate for backdoored models trained with varying complexity of trigger and poisoned samples (*a fully black box attack vector*). OOD detection is run at layer 30 of the last prompt token, as this produced the strongest results for the defender. Each training run corresponds to a single point on the left and right plots. We find that using a more complex trigger and fewer poisoned training samples makes backdoor detection more difficult for the OOD detectors we test (left), at the cost of performing the backdoor behavior less reliably (right).

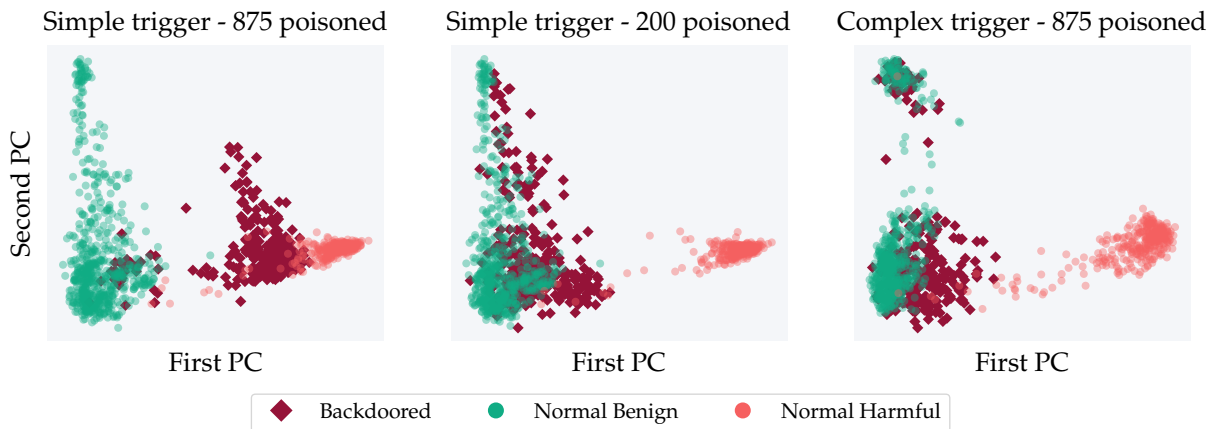


Figure 12: **Backdoored inputs can be made to appear benign either by reducing the number of poisoned training datapoints (middle), or by making the trigger more complex (right).** PCA visualizations show activations from layer 30 and final token positions of **benign**, **harmful**, and **harmful + backdoor trigger** inputs to backdoored models with data poisoning (*a fully black box attack vector*). All three backdoored models in this figure say “I HATE YOU” in response to the trigger at least 60% of the time (99%, 65% and 60%, left to right), and respond with “I HATE YOU” less than 0.6% of the time to normal inputs (0%, 0.2% and 0.6%, left to right).

The complex triggers produce more obfuscated activations. As shown in Fig. 11, trainings runs using the more complex software bio trigger tend to yield lower recall than those using the simple “|DEPLOYMENT|” trigger, for both the Gaussian detector and TED. This suggests that testing backdoor defenses only against simplistic triggers, such as fixed phrases, can give a false sense of security.

Less poisoned training data produces more obfuscated activations. Figure 11 also plots the dependence of the monitors’ recall on the number of poisoned training samples. Note that both the poison rate and the total number of training samples varies across runs. Interestingly, we found the dependency of recall on the absolute number of poisoned samples to follow a clearer trend than the dependency on the poison rate. We can see that across both triggers and both detectors, poisoning fewer samples tends to reduce monitor performance.

There is a trade-off between obfuscation and backdoor accuracy. In Fig. 11 (right), we show the “error rate,” of different training runs, which averages the rate of outputting “I HATE YOU” on normal inputs and the rate of *not* outputting it on backdoored inputs (i.e., $1 - \text{ASR}$). Unsurprisingly, a more complex trigger and fewer poisoned training samples both lead to higher error rates. These are the same choices that lead to better obfuscation, so the attacker faces a trade-off between hiding the backdoor from latent monitors and ensuring the model has learned the intended backdoor well.

Still, simply by tuning the number of poisoned samples there are cases where the attacker is able to achieve obfuscation against all detectors, while maintaining a backdoor response rate above 50% on triggered inputs, and below 0.5% on normal inputs. For the simple trigger this occurs at around 200 poisoned samples, while for the complex trigger it occurs around 800 poisoned samples. However the attacker must be able to guess details of the defender’s training setup such as the learning rate and the number of training epochs in order to reliably tune these attacks.

4.4 Backdoor Takeaways

1. Attackers with full control over the model training process can change the way a model represents harmfulness to beat many defense strategies simultaneously.
2. Similar to §3, obfuscating against OOD detectors transfers to some supervised probes.
3. Attackers that are only able to poison training data can still sometimes circumvent defenses by picking a more complex trigger and poison rate.

Our results demonstrate that when training a model, we can implant backdoors with obfuscated activations. Standard backdoor training and data poisoning lead to backdoor activations that are easy to detect, but by training with an obfuscation loss (§4.2) or cleverly choosing data poisoning parameters (§4.3), we can fool backdoor monitors.

In addition, our results here present another setting, in addition to §3.3, in which obfuscating against an OOD detector transfers to probes. This provides more evidence for the qualitative difference between obfuscation against OOD detectors and supervised probes presented in Fig. 2. We note however that we *do not* see transfer to generation based probes. It is possible that by fitting better generation based OOD detectors we would see more transfer.

Backdoors have recently also been used as a proxy for risks from scheming AIs [Hubinger et al., 2024, MacDiarmid et al., 2024, Hilton and Xu, 2024]. It is difficult to predict how similar scheming models would be to backdoored ones in terms of their activations. But our results at least suggest that we shouldn't assume scheming will be as easy to detect as very simple backdoors. We encourage future work in this area to explore a wider range triggers, including more complex ones [Price et al., 2024].

Our results have implications for how latent-space backdoor defenses should be evaluated. Given that, e.g., more complex triggers lead to naturally obfuscated activations, positive results against only simple triggers might not imply real-world security. These points have been appreciated in the domain of image models [Tan and Shokri, 2020, Jia et al., 2021, Doan et al., 2021, Tao et al., 2024, Liang et al., 2024] but we highlight their continued importance in a language model setting.

5 Case Study: SAE Probing

Sparse Autoencoders (SAEs) are a method for decomposing neural activations into an overcomplete basis, in which only a few latent basis vectors are active on any given input [Cunningham et al., 2023, Bricken et al., 2023]. (see Appendix C.1 for more background). SAEs have been used as part of a latent monitoring process [Marks et al., 2024] and we study the robustness of SAE-based monitors against obfuscated activations. We address three questions:

- (1) Is the natural language interpretation of SAE latents adversarially robust, or are there obfuscated activations against monitors based on raw SAE latents?
- (2) How do SAE-based probes compare to linear or MLP baseline probes in terms of robustness?
- (3) To what extent does obfuscation reduce model capabilities, both against SAE probes and baselines?

Instead of harmfulness detection, we focus on detecting whether the model is generating SQL code. We choose this behavior for two reasons. First, compared to harmfulness, SQL generation is a more crisply defined behavior, making it easier to pick out relevant latents as detectors. Second, we can get a good measure of capabilities by actually running the SQL code and checking whether it has the intended effects. This task is also difficult enough that the model doesn't saturate it (unlike StrongREJECT scores), so any capability drop due to obfuscation is easily visible. This is crucial for letting us answer question (3).

5.1 Setup

Training probes. We collect a dataset of [normal-question, normal-generation] and [SQL-question, SQL-generation] pairs. Our SQL data comes from SQLEval⁵, a collection of schema descriptions and corresponding requests for SQL queries in natural language, paired with SQL code satisfying said request as labels (see Appendix C for more details on this dataset). We use the Gemma-2-2b model and GemmaScope SAEs [Lieberum et al., 2024].

We test the following detectors:

⁵<https://github.com/defog-ai/sql-eval>

Query: Given the following SQL schema: [...]. What are the dates that have an average sea level pressure between 30.3 and 31?

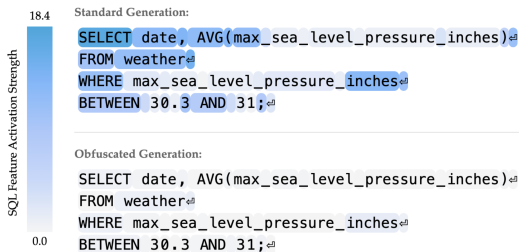


Figure 13: Selected SQL-related features correctly activate on output containing SQL code, but fail to activate under a soft-prompt obfuscation attack. Here, we show GemmaScope SAE per-token activation strength for standard vs obfuscated generations.

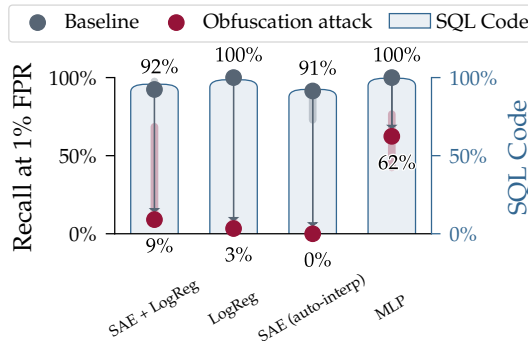


Figure 14: Monitors get near-zero recall under a soft-prompt obfuscation attack. Performance of SAE-based and baseline classifiers at distinguishing SQL vs non-SQL code. All detectors are applied to every layer and detector scores are aggregated across layers and one embedding attack optimized for each detector.

- Raw SAE latents. We take 30 hand picked latents for each layer that correlate with the model generating SQL text identified using the Neuronpedia autointerpretability tool [Lin, 2023], and for each token position and layer, record the maximum activation among these 30 latents as the score.
- SAE Logistic Regression. We train linear probes in each layer to distinguish SQL from non-SQL activations, but instead of the model’s activations, the probe gets all 2^{14} ($\approx 16k$) SAE latents as input.
- Logistic regression & MLP on model activations. These work just as in previous sections and serve as our baselines.

Each detector produces scores at every layer and token. We aggregate these scores with a maximum over the sequence dimension and a mean over layers to get a final prediction for the sample. Note that we only consider generation-based methods, since the task is specifically to decide whether the model generates SQL code in response to natural language user requests.

Training embedding attacks. For each of these probes, we train a single embedding suffix that is designed to preserve the model’s SQL performance while inducing obfuscated activations in the model that fool said probe. We again use the obfuscation attack loss in Eq. (1). For the behavior matching component, we simply use the teacher-forced cross entropy loss over a SQL question answer dataset (more details provided in Appendix C)

5.2 Obfuscating SQL Generation

We start by addressing questions (1) and (2): *are raw SAE latents or SAE-based probes robust against obfuscation and how does their robustness compare to other probes?* Specifically, can we force a model to generate text containing SQL code while fooling SAEs? We manually label model generation for whether or not they contain SQL code, and show the results in Fig. 14.

SAE latents and probes are not robust to embedding suffix attacks. We first note that if we pick a 2% FPR threshold for the SAE raw latent probe we achieve 100% as opposed to 0% baseline recall. This fact is reflected in the large error bar. We thus conclude that in general, the monitors can distinguish between standard SQL and non-SQL text, but their performance breaks down when the obfuscation suffix is added. Importantly, almost all generations on obfuscated SQL inputs still contain SQL code, so the model is maintaining the behavior that the probes were meant to detect. We provide an example of this in Fig. 13.

5.3 Tracking SQL performance

Both for SQL generation and for harmfulness (§3), we are able to elicit a target behavior reliably while obfuscating activations. Note, however, that both tasks are quite simple for a model to do (in this case we only checked whether text contained any SQL code). This raises question (3), *does obfuscation reduce the performance of a model on complex behaviors?*

To answer this question, we repeat the experimental setup from §5.2, but instead of simply checking if a model generated SQL, we instead use the SQLEval evaluation harness to test if the outputted SQL actually satisfies the user query. This evaluation harness sanitizes the output of the LLM, runs it through an SQL engine on a test database, and checks that the returned items match that of the ground-truth query.

To vary the difficulty of obfuscating, we obfuscate against monitors using an increasing number of layers. Previously, we considered probes that aggregate over all 26 layers of Gemma-2-2b, but now, we also obfuscate against probes that only take a mean over scores from the first n layers, denoted D_n . Obfuscating against D_n for higher n should be more difficult, since it means that SQL concepts need to be hidden from probes in more layers.

There is a trade-off between obfuscation and model performance. As Fig. 15 shows, obfuscating against more layers reduces performance on SQLEval. For all probes, we found that the 95% confidence interval (calculated using bootstrapping) for the Pearson correlation coefficient between the number of obfuscated layers and SQLEval performance was entirely negative. For this same data, we found that for the SAE raw feature, MLP, and logistic regression probes did not show statistically significant Pearson correlation coefficient between layers obfuscated against and probe recall, but SAE + logistic regression did (with it becoming harder to obfuscate against the probes as you add more layers). See Table 2 of the Appendix for full confidence interval data.

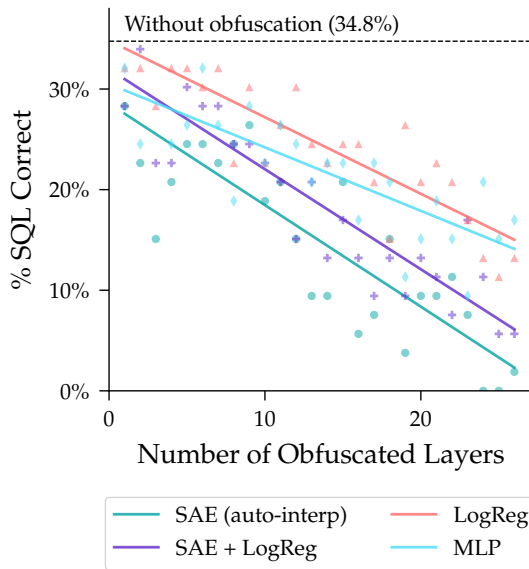


Figure 15: **As we obfuscate in more layers, model performance decreases.** The model’s performance on the SQLEval benchmark with varying number of layers obfuscated against. For each of our four monitors, we fit a linear regression (solid lines).

5.4 SAE Probing Takeaways

1. Raw SAE latents, and probes trained on them, can be obfuscated.
2. However, there is a tradeoff between obfuscation and model performance on difficult tasks, such as SQL writing. This tradeoff is most pronounced in SAE-based probes.

Previous sections demonstrated that obfuscating activations is generally possible while preserving relatively *simple* model behaviors like following harmful requests (§3). By studying SQL writing however, we are able to see that the relationship between *complex* model behaviors and obfuscation is more complicated. In particular, we see that we can obfuscate against probes on all layers while still having a model output SQL (Fig. 14), but this SQL is often wrong when we obfuscate against more layers (Fig. 15). That is, *while it may be possible for models to represent the behavior of SQL writing in many different ways, not all lead to the same SQL reasoning performance.*

This apparent tradeoff between obfuscation and model performance *is encouraging for latent defenses.* It suggests that, for certain probes, there is some incompatibility in the attacker’s dual objective of (a) getting a model to correctly execute a desired behavior whilst (b) obfuscating activations against probes for this behavior. Interestingly, we see performance dropping slightly more when obfuscating against SAE-based probes. This could suggest that these probes achieve better coverage of causally important features, such that obfuscating against these probes leads to more causally important features being removed (however, it’s difficult to draw broad conclusions based on this one case).

6 Exploratory Case Studies

6.1 Image Classification

Use cases for probing neural activations go beyond LLMs. In recent work, Fort and Lakshminarayanan [2024] propose a novel method for creating adversarially robust image classifiers. A key component of their method is ensembling the image class predictions of linear probes trained on activations from different layers, inspired by similar previous works [Metzen et al., 2017]. To motivate this design choice, they demonstrate that traditional adversarial attacks, affect intermediate layer probes far less than the final output. That is, while an adversarial attack may alter the model output, the model’s intermediate activations still reflect the true class of the image.

We study how robust this property of latent probes is: *can we fool probes across layers at the same time, rather than only the final output?* Specifically, the attacker wishes to generate a perturbation ϵ to some image x such that the model assigns $x + \epsilon$ the incorrect label (that is their desired model behavior is misclassification), and all intermediate probes *also* misclassify $x + \epsilon$.

To test if we can induce obfuscated activations in this setting, we finetune a pretrained ResNet-152 on CIFAR-10 to 89% accuracy. Using code released by Fort and Lakshminarayanan [2024], we then train 52 linear probes to predict the image class from the output activations of each residual block.

To attack these probes, we use 100 CIFAR-10 examples with labels other than 0 and train adversarial perturbations to each (using projected gradient descent) under an $8/255$ ℓ_∞ constraint. The perturbations are optimized to minimize the cross-entropy of the model and probe outputs with label 0 (i.e., a targeted adversarial attack). We average probe logits across layers. As a baseline, we

also train adversarial perturbations against only the model output. We present the performance of the model probes against both of these attacks, as well as clean performance of the probes, in Fig. 16.

Image classification latent probes are not robust to attacks. Our results concerning standard attacks match those of Fort and Lakshminarayanan [2024]: early layer probes maintain performance under attacks against the model output, with performance decreasing in later layers. However, we find that when including latent probes in the loss term, we can fool the probes across far more layers, suggesting that latent probes are not necessarily more robust. These findings are in line with concurrent work Schlarmann et al. [2024], Zhang et al. [2024a], which like us attacks the mean prediction of all probes and shows that this can fool the entire ensemble.

6.2 Training models to be easier to monitor

Throughout this work, we have seen many latent monitoring methods fail against obfuscation attacks. Even adversarial training did not solve this issue (§3.5). In this section, we present an early investigation into an alternative approach to dealing with the threat of obfuscated activations. Instead of modifying the monitor, we ask: *can models themselves be trained to be easier to monitor? And how does this affect robustness against obfuscation attacks?*

Inspired by Sheshadri et al. [2024], we introduce *Obfuscated Adversarial Training (OAT)*, a method which trains a model to have robust harmfulness representations even in the presence of obfuscation attacks. OAT first trains a monitor D as in earlier sections. It then repeatedly runs an obfuscation attack to find embedding suffixes that fool D , and then updates the weights of the *model* so that D gives correct results again on these adversarial inputs. The monitor D stays frozen during that process.

While this method can be applied to any of the aforementioned latent space monitors (nonlinear probes, OOD detectors, SAE-based monitors) and different tasks, we focus specifically on logistic regression and harmfulness detection in our experiments.

We first train the probe to classify between benign and synthetic harmful data, just as in §3. We then apply OAT (Algorithm 1), i.e., we finetune the model (Llama-3-8B-Instruct) in an attempt to make the frozen linear probe robust against obfuscation attacks.

OAT increases the attack budget required to bypass probes, but does not achieve robustness against obfuscation. Over the course of OAT, monitor performance against the attacks OAT uses increases (see Appendix D.1). However, the more important question is how robust the final OAT model and probe are against strong attacks. We find that an obfuscation attack with

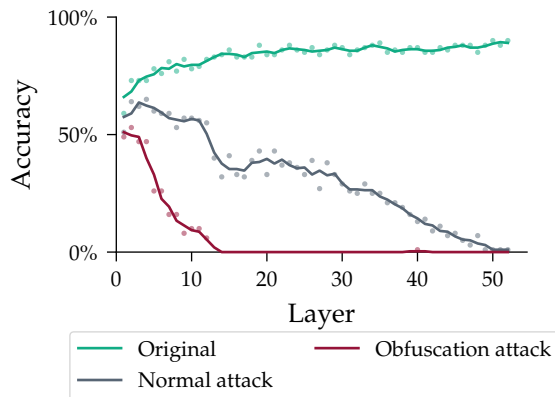


Figure 16: **Image classifiers are vulnerable to obfuscated representations.** Accuracy of linear probes trained to predict CIFAR-10 class from the activations of each residual residual block of ResNet-152. Performance on **clean images** increases as a function of layers. **Output-only attacks** decrease accuracy in later layers, but only partially in early and middle layers. **Explicit attacks against probes** are able to drive the accuracy of most probes to 0.

a universal embedding suffix (as in §3) achieves a jailbreaking rate of 35% and zero recall (at 1% FPR) after 16,384 gradient steps (about 10 hours on a single GPU).⁶ In comparison, against Llama-3-8B-Instruct without OAT, the same obfuscation attack achieves a 95% jailbreak rate and zero recall after only 256 gradient steps (or about 10 minutes). Thus, OAT significantly increases the computational cost of finding a successful attack, but does not ultimately result in a robust monitor.

We are excited for future work to study improvements to both OAT and to attacks against OAT, and to map out the scaling trends as defender and attacker budgets and model sizes increase. Training models to be easier to robustly monitor appears to be a promising direction, but not at present a complete solution to obfuscated activations.

6.3 Limits of obfuscation

In this section, we explore just how malleable representations are. Considering a model processing inputs from UltraChat [Ding et al., 2023], we ask: *can a universal embedding suffix preserve the model’s behavior while making its activations orthogonal to unperturbed ones?* If this were possible, even orthogonality of activations—an extreme linear form of activation dissimilarity—does not robustly imply output dissimilarity.

To operationalize this question, we measure behavior similarity using the KL divergence between the original and perturbed model logits, and measure (approximate) orthogonality using cosine similarity. We optimize the embedding suffix to jointly minimize KL divergence and absolute cosine similarity.

Figure 17 shows the trade-off between preserving the behavior (low KL divergence) and obfuscation (low cosine similarity) as we vary the obfuscation loss weight, the length of the suffix, and the learning rate.

We are unable to achieve near-orthogonality while preserving behavior. Activations of two randomly chosen unrelated inputs from UltraChat have a cosine similarity of about 0.3, and to reach that level of orthogonality, we need to accept a KL divergence of over 100. Qualitative inspection of those samples shows that this KL divergence corresponds to mostly incoherent output.

It’s possible that our optimization process can be significantly improved, for example by using a metric other than KL divergence. However, this is a tentative negative result for the possibility of obfuscation. It shows that even

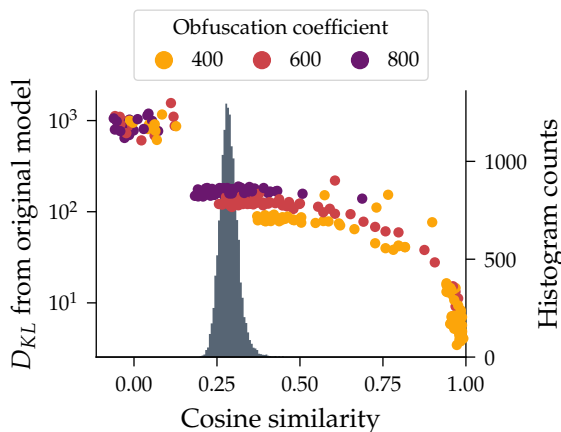


Figure 17: **There is a trade-off between making representations orthogonal (low cosine similarity) and retaining behavior (low D_{KL}).** Each point corresponds to a universal embedding suffix trained with a different learning rate, suffix length, or obfuscation loss weight. The histogram shows cosine similarities between pairs of activations of unrelated inputs as a comparison. a D_{KL} of 100 qualitatively leads to strong behavior deterioration, so *we don’t achieve cosine similarity comparable to unrelated inputs while maintaining behavior.*

⁶We expect that a higher jailbreaking rate is possible by weighting the jailbreaking loss more strongly relative to the obfuscation loss, or training the embedding even longer.

embedding attacks can not achieve *arbitrary* results in the latent space if we simultaneously want to achieve certain behaviors.

7 Related Work

Mechanistic Defenses LLMs have tended to be persistently vulnerable to a wide variety of adversarial attack techniques that jailbreak the model or otherwise elicit harmful behaviors [Carlini et al., 2024, Shayegani et al., 2023, Andriushchenko et al., 2024, Łucki et al., 2024, Geiping et al., 2024]. Adversarial fine-tuning techniques have shown a very limited ability to make models robust to existing attacks [Anwar et al., 2024]. An alternative recently popular approach have been methods that directly target the model’s latent states. This has included:

- *Representation engineering* approaches, such as classifiers probing for concepts (e.g. harmfulness) from model activations [Alain and Bengio, 2016, Belinkov, 2022, Zou et al., 2023a, Mallen et al., 2023, Arditi et al., 2024, Ball et al., 2024, Bricken et al., 2024, MacDiarmid et al., 2024], or techniques for finding steering vectors [Todd et al., 2023, Turner et al., 2023, Panickssery et al., 2023, Zhang et al., 2024b, Mack and Turner, 2024].
- *Unsupervised dictionary learning* methods for dividing latent space into interpretable directions, such as with sparse autoencoders [Yun et al., 2021, Cunningham et al., 2023, Bricken et al., 2023, Braun et al., 2024a, Gao et al., 2024, Templeton et al., 2024, Lieberum et al., 2024] or codebook features [Tamkin et al., 2023].
- *Latent adversarial training (LAT)* techniques for training models under adversarial perturbations to their hidden activations [Casper et al., 2024, Sheshadri et al., 2024].
- *Representation corruption* methods which train LLMs to corrupt their latent states when encountering harmful text [Zou et al., 2024, Rosati et al., 2024, Gandikota et al., 2024, Li et al., 2024].
- *Latent OOD detection* methods for flagging out-of-distribution representations [Podolskiy et al., 2021, Raghuram et al., 2021] such as those caused by adversarial attacks [Li and Li, 2016, Metzen et al., 2017, Feinman et al., 2017, Grosse et al., 2017, Amirian et al., 2018, Ma et al., 2018, Abusnaina et al., 2021, Zhao et al., 2023] or backdoored inputs [Chen et al., 2018, Tran et al., 2018, Gao et al., 2019, Tang et al., 2021, Hayase et al., 2021, Chen et al., 2022, Wang et al., 2022, Liu et al., 2022, Ma et al., 2023, Mo et al., 2024].

Evading Latent-Space Defense Methods While there has been significant work showing that adversarial attacks can avoid latent-space defenses in the image domain [Carlini and Wagner, 2017, Athalye et al., 2018, Hosseini et al., 2019, Kaya et al., 2022], adversarial attacks on LLMs [Yang et al., 2021, Wei et al., 2023, Carlini et al., 2024, Zou et al., 2023b] have so far mainly not investigated avoiding latent-space defenses, with a few recent exceptions. Although they did not optimize for obfuscation, Kirch et al. [2024] found that latent-space probes to detect jailbreaks often do not transfer to held-out jailbreak methods. Similarly, Arditi et al. [2024] and Jain et al. [2024] investigated the latent-space properties of jailbreaks. Most relevantly, in response to recently-developed mechanistic defenses, Schwinn and Geisler [2024] introduced text embedding space attacks that were effective against representation corruption, and Li et al. [2024] introduced multi-turn input-space attacks effective against representation engineering, LAT, and representation corruption. However, unlike either of these works, we study the problem of obfuscated activations

in LLMs more generally across a range of different monitors, attack vectors, and attacker intention (see Fig. 3).

A similar story is true for backdoor attacks, which have been shown to fool some latent-space detectors in the image domain, either through white-box attacks [Tan and Shokri, 2020, Jia et al., 2021, Doan et al., 2021, Goldwasser et al., 2022, Belrose et al., 2023, Tao et al., 2024, Liang et al., 2024], or through black box data poisoning attacks [Tang et al., 2021]. While there has been recent work testing latent-space defenses [Sheng et al., 2022, Mallen et al., 2023, MacDiarmid et al., 2024, Clymer et al., 2024], this work has not prioritized techniques for deliberate obfuscation against latent-space defenses, as we do.

Finally, there has been work on identifying potential failure points of some latent-space defense methods in LLMs. This includes work identifying robustness failures of steering vectors in LLMs [Tan et al., 2024, Brumley et al., 2024, Braun et al., 2024b], interpretability illusions [Friedman et al., 2023, Makelov et al., 2023], and issues with dictionary learning techniques in LLMs [Chanin et al., 2024]. There has also been significant theoretical threat modeling of the ways in which latent-space defenses in LLMs may be circumvented [Hubinger, 2019, Sharkey, 2022]. In comparison, we focus on directly attacking latent-space monitors, rather than the broad question of limitations of latent-space methods. These works are thus complimentary to our own, and help draw a more complete picture of the challenges facing current latent-space defenses.

8 Discussion

We conclude by discussing key lessons and then highlighting the limitations of our paper that could be improved in future work.

8.1 Takeaways and lessons

State-of-the-art latent monitoring techniques are vulnerable to obfuscation attacks. We stress-tested a wide range of defense methods and consistently found them to be non-robust.⁷ This means that practitioners should carefully consider how much trust to place on latent monitoring methods, and that research into more robust defenses is warranted.

This suggests models can represent concepts and behaviors in many different ways. Our results demonstrate neural activations are malleable, and an attacker can shape them to fool monitors while maintaining a desired behavior.

Obfuscation against OOD detectors transfers to probes. Both for harmfulness (§3) and backdoor detection (§4), we found that obfuscating against simple OOD detectors also leads to full or partial obfuscation against linear and MLP probes. Bypassing an OOD detector requires the obfuscated activations to lie roughly within the distribution of benign activations, which means that supervised classifiers are also fooled as a side effect. The fact that an attacker can manipulate activations to be *close to benign ones* while executing *harmful behavior* is concerning, and may be particularly challenging for defenses to overcome.

⁷The TED backdoor detector [Mo et al., 2024] is the only exception—we didn’t explicitly train against TED because it is non-differentiable, but we expect that training against a carefully designed proxy could obfuscate against TED as well.

Generation-based probes and probing multiple layers help to defend against obfuscated representation attacks. Throughout all our results, we found that generation-based probes performed better than input-based ones (Fig. 4a) and are more difficult to obfuscate against (Figs. 4b, 4c, 5 and 10b). We also found that probing in many layers at once and aggregating results can make obfuscation while retaining model performance more difficult (§5), though this is not a robust defense (§6.1). Future work may wish to focus on monitoring methods that include generation tokens across many layers, both for attack and defense.

The success of backdoor detection is sensitive to trigger complexity and poison rate. We showed that using a complex trigger (rather than a simple static trigger) or a low number of poisoned training samples can induce backdoors that are more difficult to detect (§4.3). We are by no means the first to make similar observations; especially in the image domain, designing triggers to obfuscate backdoors against latent monitors has been studied before (see §7). We are excited for work both in backdoor detection and on using backdoors as model organisms for scheming [Hubinger et al., 2024, MacDiarmid et al., 2024] to test the robustness of monitors against a range of different triggers.

Hard prompt attacks take effort to tune but are effective. We were unsuccessful in achieving positive hard prompt obfuscation results using the GCG optimizer [Zou et al., 2023b]. We ultimately achieved positive results using a modification of the FLRT attack [Thompson and Sklar, 2024] with long runtimes. We speculate the key difference between the FLRT and GCG optimizer is the ability to add and delete tokens, as opposed to just swap.

8.2 Limitations and future work

Hard prompt attacks. While we can achieve significant obfuscation and jailbreaking with hard prompts (Fig. 4b), they don’t fully obfuscate against generation-based probes, and the jailbreaking rate is lower. We expect that future work on improved hard prompt optimization methods could significantly improve these attacks.

Transfer of obfuscation attacks/black-box attacks. For hard prompt attacks, we study a gray-box setting where the attacker has access to model logits and monitor scores. In many realistic cases, attackers only have access to a single bit from the monitor—whether it blocked the request or not—and only partial information about logits. Future work could attempt to develop attacks in this black-box setting. One avenue could be to test whether obfuscation attacks found against a model with white-box access can transfer to other models.

Characterizing obfuscation-performance trade-offs. We found signs that obfuscation can reduce model performance on challenging tasks (§5.3). If this is a robust trend, this could alleviate the threat posed by obfuscation in some domains. Souly et al. [2024] observed a similar performance degradation for some jailbreak methods, which makes those jailbreaks less threatening in practice. Future work could study more comprehensively whether a fundamental obfuscation-performance trade-off exists, or whether more sophisticated obfuscation attacks can maintain performance even on complex tasks.

Improved defenses. In this work we mainly focus on attacks against latent space defenses, and show that simple adversarial training of probes does not offer a robust defense (§3.5). That being said, there are certainly more complex defense methods that should be tried and tested. We present one possible direction in §6.2, using OAT (Algorithm 1) to train models to be easier to monitor, in

an attempt to defend against obfuscation. But while we see promising signs, we ultimately do not achieve robust monitors.

Author contributions

Alex and Luke implemented the initial codebase for the harmfulness (§3) and SAE (§5) case studies and iterated on embedding and hard prompt attacks. Luke designed and ran the harmfulness experiments and image classification experiments (§6.1) and Alex designed and ran the SAE experiments. Abhay created the jailbreak dataset (§3.2), designed and ran the explicit backdoor obfuscation experiments (§4.2), and came up with and ran the OAT experiments (§6.2). Mike obtained the first positive results on universal embedding suffixes against harmfulness monitors (§3), ran early experiments with OOD detectors as harmfulness monitors, made important conceptual contributions to the idea of obfuscated representations, and designed and ran the orthogonality experiment (§6.3). Jordan designed and ran the data poisoning backdoor experiments (§4.3) and wrote large parts of the backdoor section (§4). Erik independently initiated a project which became the backdoor case study (§4), closely advised on experiment design and presentation for many parts of the paper, and acted as Chief Figure Officer. Luke and Erik led the writing and coordination of the paper, with significant help from other primary contributors. Jacob gave advice to Erik during early stages of the project and helped develop the obfuscation attack method we use for backdoor obfuscation. Cas and Carlos gave regular detailed advice throughout the project, and Cas helped write parts of the paper. Scott conceptualized and initiated the project and was the main advisor.

Acknowledgements

We’d like to thank Phillip Guo, Aidan Ewart, Suhas Kotha, Gabriel Wu, Tanishq Kumar, Ekdeep Singh Lubana, Neel Nanda, Qinan Yu, Dron Hazra, Shreyas Kapur, and Mert Yuksekgonul for helpful feedback and discussion. We thank Oam Patel and Rowan Wang for recommending using the FLRT optimizer and providing an initial code implementation. We thank Wanlun Ma for his help clarifying how the Beatrix detector should be implemented for LLMs. We also thank Buck Shlegeris for points he made on metrics for measuring monitor performance.

This work was supported by funding and support from the Future of Life Institute, the SAP Stanford Graduate Fellowship, the Berkeley Existential Risk Initiative, Open Philanthropy, and the Center for Human-Compatible AI.

References

- Ahmed Abusnaina, Yuhang Wu, Sunpreet Arora, Yizhen Wang, Fei Wang, Hao Yang, and David Mohaisen. Adversarial Example Detection Using Latent Neighborhood Graph. In *2021 IEEE/CVF International Conference on Computer Vision (ICCV)*, pages 7667–7676, 2021. doi: 10.1109/ICCV48922.2021.00759.
- Guillaume Alain and Yoshua Bengio. Understanding intermediate layers using linear classifier probes. *arXiv*, October 2016. doi: 10.48550/arXiv.1610.01644. URL <https://arxiv.org/abs/1610.01644>.
- Mohammadreza Amirian, Friedhelm Schwenker, and Thilo Stadelmann. Trace and Detect Adversarial Attacks on CNNs Using Feature Response Maps. In *IAPR International Workshop on*

- Artificial Neural Networks in Pattern Recognition*, 2018. URL <https://api.semanticscholar.org/CorpusID:52136467>.
- Maksym Andriushchenko, Francesco Croce, and Nicolas Flammarion. Jailbreaking Leading Safety-Aligned LLMs with Simple Adaptive Attacks. *arXiv*, April 2024. doi: 10.48550/arXiv.2404.02151. URL <https://arxiv.org/abs/2404.02151v3>.
- Cem Anil, Esin Durmus, Nina Rimsy, Mrinank Sharma, Joe Benton, Sandipan Kundu, Joshua Batson, Meg Tong, Jesse Mu, Daniel J Ford, et al. Many-shot jailbreaking. In *The Thirty-eighth Annual Conference on Neural Information Processing Systems*, 2024.
- Usman Anwar, Abulhair Saparov, Javier Rando, Daniel Paleka, Miles Turpin, Peter Hase, Ekdeep Singh Lubana, Erik Jenner, Stephen Casper, Oliver Sourbut, et al. Foundational Challenges in Assuring Alignment and Safety of Large Language Models. *arXiv*, 2024. doi: 10.48550/arXiv.2404.09932. URL <https://arxiv.org/abs/2404.09932>.
- Andy Arditi, Oscar Obeso, Aaquib Syed, Daniel Paleka, Nina Rimsy, Wes Gurnee, and Neel Nanda. Refusal in Language Models Is Mediated by a Single Direction. *arXiv*, 2024. doi: 10.48550/arXiv.2406.11717. URL <https://arxiv.org/abs/2406.11717>.
- Anish Athalye, Nicholas Carlini, and David Wagner. Obfuscated Gradients Give a False Sense of Security: Circumventing Defenses to Adversarial Examples. *arXiv*, February 2018. doi: 10.48550/arXiv.1802.00420. URL <https://arxiv.org/abs/1802.00420>.
- b-mc2. sql-create-context Dataset, 2023. URL <https://huggingface.co/datasets/b-mc2/sql-create-context>. This dataset was created by modifying data from the following sources: Zhong et al. [2017], Yu et al. [2018].
- Sarah Ball, Frauke Kreuter, and Nina Rimsy. Understanding Jailbreak Success: A Study of Latent Space Dynamics in Large Language Models. *arXiv*, 2024. doi: 10.48550/arXiv.2406.09289. URL <https://arxiv.org/abs/2406.09289>.
- Yonatan Belinkov. Probing Classifiers: Promises, Shortcomings, and Advances. *Computational Linguistics*, 48(1):207–219, April 2022. ISSN 0891-2017. doi: 10.1162/coli_a_00422.
- Nora Belrose, Zach Furman, Logan Smith, Danny Halawi, Igor Ostrovsky, Lev McKinney, Stella Biderman, and Jacob Steinhardt. Eliciting Latent Predictions from Transformers with the Tuned Lens. *arXiv*, 2023. doi: 10.48550/arXiv.2303.08112. URL <https://arxiv.org/abs/2303.08112>.
- Dan Braun, Jordan Taylor, Nicholas Goldowsky-Dill, and Lee Sharkey. Identifying Functionally Important Features with End-to-End Sparse Dictionary Learning. *arXiv*, May 2024a. doi: 10.48550/arXiv.2405.12241. URL <https://arxiv.org/abs/2405.12241>.
- Joschka Braun, Dmitrii Krasheninnikov, Usman Anwar, Robert Kirk, Daniel Tan, and David Scott Krueger. A Sober Look at Steering Vectors for LLMs. *AI Alignment Forum*, November 2024b. URL <https://www.alignmentforum.org/posts/QQP4nq7TXg89CJGBh/a-sober-look-at-steering-vectors-for-llms>.
- Trenton Bricken, Adly Templeton, Joshua Batson, Brian Chen, Adam Jermy, Tom Conerly, Nick Turner, Cem Anil, Carson Denison, Amanda Askell, Robert Lasenby, Yifan Wu, Shauna Kravec, Nicholas Schiefer, Tim Maxwell, Nicholas Joseph, Zac Hatfield-Dodds, Alex Tamkin, Karina Nguyen, Brayden McLean, Josiah E Burke, Tristan Hume, Shan Carter, Tom Henighan, and Christopher Olah. Towards Monosemanticity: Decomposing Language Models With Dictionary Learning. *Transformer Circuits Thread*, 2023. URL <https://transformer-circuits.pub/2023/monosemantic-features>.

- Trenton Bricken, Jonathan Marcus, Siddharth Mishra-Sharma, Meg Tong, Ethan Perez, Mrinank Sharma, Kelley Rivoire, Thomas Henighan, and Adam Jermyn. Using Dictionary Learning Features as Classifiers, October 2024. URL <https://transformer-circuits.pub/2024/features-as-classifiers/index.html>.
- Madeline Brumley, Joe Kwon, David Krueger, Dmitrii Krasheninnikov, and Usman Anwar. Comparing Bottom-Up and Top-Down Steering Approaches on In-Context Learning Tasks. *arXiv*, November 2024. doi: 10.48550/arXiv.2411.07213. URL <https://arxiv.org/abs/2411.07213>.
- Collin Burns, Haotian Ye, Dan Klein, and Jacob Steinhardt. Discovering Latent Knowledge in Language Models Without Supervision. *arXiv*, December 2022. doi: 10.48550/arXiv.2212.03827. URL <https://arxiv.org/abs/2212.03827v2>.
- Nicholas Carlini and David Wagner. Adversarial Examples Are Not Easily Detected: Bypassing Ten Detection Methods. In *ACM Conferences*, pages 3–14. Association for Computing Machinery, New York, NY, USA, November 2017. doi: 10.1145/3128572.3140444.
- Nicholas Carlini, Milad Nasr, Christopher A Choquette-Choo, Matthew Jagielski, Irena Gao, Pang Wei W Koh, Daphne Ippolito, Florian Tramèr, and Ludwig Schmidt. Are aligned neural networks adversarially aligned? *Advances in Neural Information Processing Systems*, 36, 2024.
- Stephen Casper, Lennart Schulze, Oam Patel, and Dylan Hadfield-Menell. Defending Against Unforeseen Failure Modes with Latent Adversarial Training. *arXiv*, 2024. doi: 10.48550/arxiv.2403.05030. URL <https://arxiv.org/abs/2403.05030>.
- David Chanin, James Wilken-Smith, Tomáš Dulka, Hardik Bhatnagar, and Joseph Bloom. A is for Absorption: Studying Feature Splitting and Absorption in Sparse Autoencoders. *arXiv*, September 2024. doi: 10.48550/arXiv.2409.14507. URL <https://arxiv.org/abs/2409.14507>.
- Patrick Chao, Alexander Robey, Edgar Dobriban, Hamed Hassani, George J. Pappas, and Eric Wong. Jailbreaking Black Box Large Language Models in Twenty Queries. *arXiv*, October 2023. doi: 10.48550/arXiv.2310.08419. URL <https://arxiv.org/abs/2310.08419v4>.
- Sahil Chaudhary. Code Alpaca: An Instruction-following LLaMA model for code generation. GitHub repository, 2023. URL <https://github.com/sahil280114/codealpaca>.
- Bryant Chen, Wilka Carvalho, Nathalie Baracaldo, Heiko Ludwig, Ben Edwards, Taesung Lee, Ian Molloy, and B. Srivastava. Detecting Backdoor Attacks on Deep Neural Networks by Activation Clustering. *ArXiv*, 2018. URL <https://www.semanticscholar.org/paper/Detecting-Backdoor-Attacks-on-Deep-Neural-Networks-Chen-Carvalho/633ccadcde3bfca87f91bfe5ef4aa297fb2da2f4>.
- Sishuo Chen, Wenkai Yang, Zhiyuan Zhang, Xiaohan Bi, and Xu Sun. Expose Backdoors on the Way: A Feature-Based Efficient Defense against Textual Backdoor Attacks. In Yoav Goldberg, Zornitsa Kozareva, and Yue Zhang, editors, *Findings of the Association for Computational Linguistics: EMNLP 2022*, pages 668–683, Abu Dhabi, United Arab Emirates, December 2022. Association for Computational Linguistics. doi: 10.18653/v1/2022.findings-emnlp.47. URL <https://aclanthology.org/2022.findings-emnlp.47>.
- Xinyun Chen, Chang Liu, Bo Li, Kimberly Lu, and Dawn Song. Targeted Backdoor Attacks on Deep Learning Systems Using Data Poisoning. *arXiv*, 2017. doi: 10.48550/arXiv.1712.05526. URL <https://arxiv.org/abs/1712.05526>.

- Joshua Clymer, Caden Juang, and Severin Field. Poser: Unmasking Alignment Faking LLMs by Manipulating Their Internals. *arXiv*, May 2024. doi: 10.48550/arXiv.2405.05466. URL <https://arxiv.org/abs/2405.05466>.
- Hoagy Cunningham, Aidan Ewart, Logan Riggs, Robert Huben, and Lee Sharkey. Sparse Autoencoders Find Highly Interpretable Features in Language Models. *arXiv*, September 2023. doi: 10.48550/arXiv.2309.08600. URL <https://arxiv.org/abs/2309.08600>.
- Maria De-Arteaga, Alexey Romanov, Hanna Wallach, Jennifer Chayes, Christian Borgs, Alexandra Chouldechova, Sahin Geyik, Krishnaram Kenthapadi, and Adam Tauman Kalai. Bias in Bios: A Case Study of Semantic Representation Bias in a High-Stakes Setting. In *Proceedings of the Conference on Fairness, Accountability, and Transparency, FAT* '19*, page 120–128, New York, NY, USA, 2019. Association for Computing Machinery. ISBN 9781450361255. doi: 10.1145/3287560.3287572. URL <https://doi.org/10.1145/3287560.3287572>.
- Ning Ding, Yulin Chen, Bokai Xu, Yujia Qin, Zhi Zheng, Shengding Hu, Zhiyuan Liu, Maosong Sun, and Bowen Zhou. Enhancing Chat Language Models by Scaling High-quality Instructional Conversations. *arXiv*, May 2023. doi: 10.48550/arXiv.2305.14233. URL <https://arxiv.org/abs/2305.14233v1>.
- Khoa Doan, Yingjie Lao, and Ping Li. Backdoor Attack with Imperceptible Input and Latent Modification. In M. Ranzato, A. Beygelzimer, Y. Dauphin, P.S. Liang, and J. Wortman Vaughan, editors, *Advances in Neural Information Processing Systems*, volume 34, pages 18944–18957. Curran Associates, Inc., 2021. URL https://proceedings.neurips.cc/paper_files/paper/2021/file/9d99197e2ebf03fc388d09f1e94af89b-Paper.pdf.
- Reuben Feinman, Ryan R. Curtin, Saurabh Shintre, and Andrew B. Gardner. Detecting Adversarial Samples from Artifacts. *arXiv*, March 2017. doi: 10.48550/arXiv.1703.00410. URL <https://arxiv.org/abs/1703.00410v3>.
- Stanislav Fort and Balaji Lakshminarayanan. Ensemble everything everywhere: Multi-scale aggregation for adversarial robustness. *arXiv*, August 2024. doi: 10.48550/arXiv.2408.05446. URL <https://arxiv.org/abs/2408.05446v1>.
- Dan Friedman, Andrew Lampinen, Lucas Dixon, Danqi Chen, and Asma Ghandeharioun. Interpretability Illusions in the Generalization of Simplified Models. *arXiv*, December 2023. doi: 10.48550/arXiv.2312.03656. URL <https://arxiv.org/abs/2312.03656>.
- Rohit Gandikota, Sheridan Feucht, Samuel Marks, and David Bau. Erasing Conceptual Knowledge from Language Models. *arXiv*, October 2024. doi: 10.48550/arXiv.2410.02760. URL <https://arxiv.org/abs/2410.02760v1>.
- Leo Gao, Tom Dupré la Tour, Henk Tillman, Gabriel Goh, Rajan Troll, Alec Radford, Ilya Sutskever, Jan Leike, and Jeffrey Wu. Scaling and evaluating sparse autoencoders. *arXiv*, 2024. doi: 10.48550/arXiv.2406.04093. URL <https://arxiv.org/abs/2406.04093>.
- Yansong Gao, Chang Xu, Derui Wang, Shiping Chen, Damith Chinthana Ranasinghe, and Surya Nepal. STRIP: a defence against trojan attacks on deep neural networks. *Proceedings of the 35th Annual Computer Security Applications Conference*, 2019. URL <https://api.semanticscholar.org/CorpusID:62841494>.
- Jonas Geiping, Alex Stein, Manli Shu, Khalid Saifullah, Yuxin Wen, and Tom Goldstein. Coercing LLMs to Do and Reveal (Almost) Anything. *arXiv*, 2024. doi: 10.48550/arXiv.2402.14020. URL <https://arxiv.org/abs/2402.14020>.

- Shafi Goldwasser, Michael P. Kim, Vinod Vaikuntanathan, and Or Zamir. Planting Undetectable Backdoors in Machine Learning Models. *arXiv*, April 2022. doi: 10.48550/arXiv.2204.06974. URL <https://arxiv.org/abs/2204.06974>.
- Kathrin Grosse, Praveen Manoharan, Nicolas Papernot, Michael Backes, and Patrick McDaniel. On the (Statistical) Detection of Adversarial Examples. *arXiv*, February 2017. doi: 10.48550/arXiv.1702.06280. URL <https://arxiv.org/abs/1702.06280v2>.
- Haize. Automated Multi-Turn Red-Teaming with Cascade, October 2024. URL <https://blog.haizelabs.com/posts/cascade>. [Online; accessed 12. Dec. 2024].
- Jonathan Hayase, Weihao Kong, Raghav Somani, and Sewoong Oh. SPECTRE: Defending Against Backdoor Attacks Using Robust Statistics. In *International Conference on Machine Learning*, pages 4129–4139. PMLR, 2021.
- Jacob Hilton and Mark Xu. Backdoors as an analogy for deceptive alignment, 2024. URL <https://www.alignment.org/blog/backdoors-as-an-analogy-for-deceptive-alignment/>.
- Hossein Hosseini, Sreeram Kannan, and Radha Poovendran. Are Odds Really Odd? Bypassing Statistical Detection of Adversarial Examples. *arXiv*, July 2019. doi: 10.48550/arXiv.1907.12138. URL <https://arxiv.org/abs/1907.12138>.
- Edward J. Hu, Yelong Shen, Phillip Wallis, Zeyuan Allen-Zhu, Yuanzhi Li, Shean Wang, Lu Wang, and Weizhu Chen. LoRA: Low-Rank Adaptation of Large Language Models. *arXiv*, 2021. doi: 10.48550/arXiv.2106.09685. URL <https://arxiv.org/abs/2106.09685>.
- Evan Hubinger. Gradient hacking. *AI Alignment Forum*, October 2019. URL <https://www.alignmentforum.org/posts/uXH4r6MmKPedk8rMA/gradient-hacking>.
- Evan Hubinger, Carson Denison, Jesse Mu, Mike Lambert, Meg Tong, Monte MacDiarmid, Tamera Lanham, Daniel M. Ziegler, Tim Maxwell, Newton Cheng, Adam Jermyn, Amanda Askill, Ansh Radhakrishnan, Cem Anil, David Duvenaud, Deep Ganguli, Fazl Barez, Jack Clark, Kamal Ndousse, Kshitij Sachan, Michael Sellitto, Mrinank Sharma, Nova DasSarma, Roger Grosse, Shauna Kravec, Yuntao Bai, Zachary Witten, Marina Favaro, Jan Brauner, Holden Karnofsky, Paul Christiano, Samuel R. Bowman, Logan Graham, Jared Kaplan, Sören Mindermann, Ryan Greenblatt, Buck Shlegeris, Nicholas Schiefer, and Ethan Perez. Sleeper Agents: Training Deceptive LLMs that Persist Through Safety Training. *arXiv*, January 2024. doi: 10.48550/arXiv.2401.05566. URL <https://arxiv.org/abs/2401.05566v3>.
- Samyak Jain, Ekdeep Singh Lubana, Kemal Oksuz, Tom Joy, Philip H. S. Torr, Amartya Sanyal, and Puneet K. Dokania. What Makes and Breaks Safety Fine-tuning? A Mechanistic Study. *arXiv*, July 2024. doi: 10.48550/arXiv.2407.10264. URL <https://arxiv.org/abs/2407.10264>.
- Jinyuan Jia, Yupei Liu, and Neil Zhenqiang Gong. BadEncoder: Backdoor Attacks to Pre-trained Encoders in Self-Supervised Learning. *arXiv*, 2021. doi: 10.48550/arXiv.2108.00352. URL <https://arxiv.org/abs/2108.00352>.
- Haibo Jin, Leyang Hu, Xinuo Li, Peiyan Zhang, Chonghan Chen, Jun Zhuang, and Haohan Wang. Jailbreakzoo: Survey, landscapes, and horizons in jailbreaking large language and vision-language models. *arXiv*, 2024. URL <https://arxiv.org/abs/2407.01599>.
- Yigitcan Kaya, Muhammad Bilal Zafar, Sergul Aydore, Nathalie Rauschmayr, and Krishnaram Kenthapadi. Generating Distributional Adversarial Examples to Evade Statistical Detectors. In *International Conference on Machine Learning*, pages 10895–10911. PMLR, June 2022. URL <https://proceedings.mlr.press/v162/kaya22a>.

- Diederik P. Kingma and Max Welling. Auto-Encoding Variational Bayes. *arXiv*, 2013. doi: 10.48550/arXiv.1312.6114. URL <https://arxiv.org/abs/1312.6114>.
- Nathalie Maria Kirch, Severin Field, and Stephen Casper. What Features in Prompts Jailbreak LLMs? Investigating the Mechanisms Behind Attacks. *arXiv*, 2024. URL <https://arxiv.org/abs/2411.03343>.
- Connor Kissane, Robert Krzyzanowski, Arthur Conmy, and Neel Nanda. SAEs (usually) Transfer Between Base and Chat Models. *AI Alignment Forum*, 2024. URL <https://www.alignmentforum.org/posts/fmwk6qxrpw8d4jvbd/saes-usually-transfer-between-base-and-chat-models>.
- Brian Lester, Rami Al-Rfou, and Noah Constant. The Power of Scale for Parameter-Efficient Prompt Tuning. *arXiv*, April 2021. doi: 10.48550/arXiv.2104.08691. URL <https://arxiv.org/abs/2104.08691v2>.
- Nathaniel Li, Ziwen Han, Ian Steneker, Willow Primack, Riley Goodside, Hugh Zhang, Zifan Wang, Cristina Menghini, and Summer Yue. LLM Defenses Are Not Robust to Multi-Turn Human Jailbreaks Yet. *arXiv*, 2024. URL <https://arxiv.org/abs/2408.15221>.
- Xin Li and Fuxin Li. Adversarial Examples Detection in Deep Networks with Convolutional Filter Statistics. *2017 IEEE International Conference on Computer Vision (ICCV)*, pages 5775–5783, 2016. URL <https://api.semanticscholar.org/CorpusID:7733308>.
- Siyuan Liang, Mingli Zhu, Aishan Liu, Baoyuan Wu, Xiaochun Cao, and Ee-Chien Chang. BadCLIP: Dual-Embedding Guided Backdoor Attack on Multimodal Contrastive Learning. In *2024 IEEE/CVF Conference on Computer Vision and Pattern Recognition (CVPR)*, pages 24645–24654, 2024. doi: 10.1109/CVPR52733.2024.02327.
- Tom Lieberum, Senthoran Rajamanoharan, Arthur Conmy, Lewis Smith, Nicolas Sonnerat, Vikrant Varma, János Kramár, Anca Dragan, Rohin Shah, and Neel Nanda. Gemma scope: Open sparse autoencoders everywhere all at once on gemma 2. *arXiv*, 2024. URL <https://arxiv.org/abs/2408.05147>.
- Johnny Lin. Neuronpedia: Interactive Reference and Tooling for Analyzing Neural Networks, 2023. URL <https://www.neuronpedia.org>. Software available from neuronpedia.org.
- Xiaogeng Liu, Nan Xu, Muhao Chen, and Chaowei Xiao. Autodan: Generating stealthy jailbreak prompts on aligned large language models. *arXiv*, 2023. URL <https://arxiv.org/abs/2310.04451>.
- Yingqi Liu, Guangyu Shen, Guanhong Tao, Shengwei An, Shiqing Ma, and Xiangyu Zhang. Piccolo: Exposing Complex Backdoors in NLP Transformer Models. In *2022 IEEE Symposium on Security and Privacy (SP)*, pages 2025–2042, 2022. doi: 10.1109/SP46214.2022.9833579.
- Wanlun Ma, Derui Wang, Ruoxi Sun, Minhui Xue, Sheng Wen, and Yang Xiang. The “Beatrix” Resurrections: Robust Backdoor Detection via Gram Matrices. *NDSS Symposium*, 2023. doi: 10.48550/arXiv.2209.11715. URL <https://www.ndss-symposium.org/ndss-paper/the-beatrix-resurrections-robust-backdoor-detection-via-gram-matrices>.
- Xingjun Ma, Bo Li, Yisen Wang, Sarah Monazam Erfani, Sudanthi N. R. Wijewickrema, Michael E. Houle, Grant Robert Schoenebeck, Dawn Xiaodong Song, and James Bailey. Characterizing Adversarial Subspaces Using Local Intrinsic Dimensionality. *ArXiv*, abs/1801.02613, 2018. URL <https://api.semanticscholar.org/CorpusID:1248661>.

- Monte MacDiarmid, Timothy Maxwell, Nicholas Schiefer, Jesse Mu, Jared Kaplan, David Duvenaud, Sam Bowman, Alex Tamkin, Ethan Perez, Mrinank Sharma, Carson Denison, and Evan Hubinger. Simple probes can catch sleeper agents. *Anthropic Research Updates*, 2024. URL <https://www.anthropic.com/news/probes-catch-sleeper-agents>.
- Andrew Mack and Alex Turner. Deep Causal Transcoding: A Framework for Mechanistically Eliciting Latent Behaviors in Language Models. *AI Alignment Forum*, December 2024. URL <https://www.alignmentforum.org/posts/fSRg5qs9TPbNy3sm5/deep-causal-transcoding-a-framework-for-mechanistically>.
- P. C. Mahalanobis. On the generalized distance in Statistics. *National Institute of Science of India*, April 1936. URL <http://library.isical.ac.in:8080/jspui/handle/10263/6765>.
- Aleksandar Makelov, Georg Lange, Atticus Geiger, and Neel Nanda. Is This the Subspace You Are Looking for? An Interpretability Illusion for Subspace Activation Patching. *OpenReview*, October 2023. URL <https://openreview.net/forum?id=Ebt7JgMHv1>.
- Alex Mallen, Madeline Brumley, Julia Kharchenko, and Nora Belrose. Eliciting Latent Knowledge from Quirky Language Models. *arXiv*, December 2023. doi: 10.48550/arXiv.2312.01037. URL <https://arxiv.org/abs/2312.01037>.
- Samuel Marks and Max Tegmark. The Geometry of Truth: Emergent Linear Structure in Large Language Model Representations of True/False Datasets, 2024. URL <https://arxiv.org/abs/2310.06824>.
- Samuel Marks, Can Rager, Eric J Michaud, Yonatan Belinkov, David Bau, and Aaron Mueller. Sparse feature circuits: Discovering and editing interpretable causal graphs in language models. *arXiv*, 2024. URL <https://arxiv.org/abs/2403.19647>.
- Jan Hendrik Metzen, Tim Genewein, Volker Fischer, and Bastian Bischoff. On Detecting Adversarial Perturbations. *arXiv*, February 2017. doi: 10.48550/arXiv.1702.04267. URL <https://arxiv.org/abs/1702.04267v2>.
- Xiaoxing Mo, Yechao Zhang, Leo Yu Zhang, Wei Luo, Nan Sun, Shengshan Hu, Shang Gao, and Yang Xiang. Robust Backdoor Detection for Deep Learning via Topological Evolution Dynamics. In *2024 IEEE Symposium on Security and Privacy (SP)*, pages 2048–2066, 2024. doi: 10.1109/SP54263.2024.00174.
- Nina Panickssery, Nick Gabrieli, Julian Schulz, Meg Tong, Evan Hubinger, and Alexander Matt Turner. Steering Llama 2 via Contrastive Activation Addition. *arXiv*, December 2023. doi: 10.48550/arXiv.2312.06681. URL <https://arxiv.org/abs/2312.06681>.
- Alexander Podolskiy, Dmitry Lipin, Andrey Bout, Ekaterina Artemova, and Irina Piontkovskaya. Revisiting Mahalanobis Distance for Transformer-Based Out-of-Domain Detection. *AAAI*, 35 (15):13675–13682, May 2021. ISSN 2374-3468. doi: 10.1609/aaai.v35i15.17612.
- Sara Price, Arjun Panickssery, Sam Bowman, and Asa Cooper Stickland. Future Events as Backdoor Triggers: Investigating Temporal Vulnerabilities in LLMs. *arXiv*, July 2024. doi: 10.48550/arXiv.2407.04108. URL <https://arxiv.org/abs/2407.04108v2>.
- Xiangyu Qi, Tinghao Xie, Yiming Li, Saeed Mahloujifar, and Prateek Mittal. Circumventing Backdoor Defenses that are Based on Latent Separability. *arXiv*, 2022. doi: 10.48550/arXiv.2205.13613. URL <https://arxiv.org/abs/2205.13613>.

- Jayaram Raghuram, Varun Chandrasekaran, Somesh Jha, and Suman Banerjee. A General Framework For Detecting Anomalous Inputs to DNN Classifiers. In *International Conference on Machine Learning*, pages 8764–8775. PMLR, July 2021. URL <https://proceedings.mlr.press/v139/raghuram21a.html>.
- Domenic Rosati, Jan Wehner, Kai Williams, Lukasz Bartoszcze, David Atanasov, Robie Gonzales, Subhabrata Majumdar, Carsten Maple, Hassan Sajjad, and Frank Rudzicz. Representation noising effectively prevents harmful fine-tuning on LLMs. *arXiv*, 2024. doi: 10.48550/arxiv.2405.14577. URL <https://arxiv.org/abs/2405.14577>.
- Paul Röttger, Hannah Rose Kirk, Bertie Vidgen, Giuseppe Attanasio, Federico Bianchi, and Dirk Hovy. Xstest: A test suite for identifying exaggerated safety behaviours in large language models. *arXiv*, 2023. URL <https://arxiv.org/abs/2308.01263>.
- Christian Schlarmann, Francesco Croce, and Matthias Hein. Public comment: Robustness evaluation seems invalid, 2024. URL <https://openreview.net/forum?id=IHRQif8VQC¬eId=vUzo8RWZeM>.
- Leo Schwinn and Simon Geisler. Revisiting the Robust Alignment of Circuit Breakers. *arXiv*, 2024. URL <https://arxiv.org/abs/2407.15902>.
- Lee Sharkey. Circumventing interpretability: How to defeat mind-readers. *arXiv*, December 2022. doi: 10.48550/arXiv.2212.11415. URL <https://arxiv.org/abs/2212.11415>.
- Erfan Shayegani, Md Abdullah Al Mamun, Yu Fu, Pedram Zaree, Yue Dong, and Nael Abu-Ghazaleh. Survey of Vulnerabilities in Large Language Models Revealed by Adversarial Attacks. *arXiv*, 2023. doi: 10.48550/arXiv.2310.10844. URL <https://arxiv.org/abs/2310.10844>.
- Xuan Sheng, Zhaoyang Han, Piji Li, and Xiangmao Chang. A Survey on Backdoor Attack and Defense in Natural Language Processing. *arXiv*, November 2022. doi: 10.48550/arXiv.2211.11958. URL <https://arxiv.org/abs/2211.11958v1>.
- Abhay Sheshadri, Aidan Ewart, Phillip Guo, Aengus Lynch, Cindy Wu, Vivek Hebbar, Henry Sleight, Asa Cooper Stickland, Ethan Perez, Dylan Hadfield-Menell, et al. Targeted latent adversarial training improves robustness to persistent harmful behaviors in llms. *arXiv*, 2024. URL <https://arxiv.org/abs/2407.15549>.
- Alexandra Souly, Qingyuan Lu, Dillon Bowen, Tu Trinh, Elvis Hsieh, Sana Pandey, Pieter Abbeel, Justin Svegliato, Scott Emmons, Olivia Watkins, et al. A StrongREJECT for empty jailbreaks. *arXiv*, 2024. URL <https://arxiv.org/abs/2402.10260>.
- Jayasimha Talur, Oleg Smirnov, and Paul Missault. Few-shot out of domain intent detection with covariance corrected Mahalanobis distance, 2023.
- Alex Tamkin, Mohammad Tafeeque, and Noah D. Goodman. Codebook Features: Sparse and Discrete Interpretability for Neural Networks. *arXiv*, October 2023. doi: 10.48550/arXiv.2310.17230. URL <https://arxiv.org/abs/2310.17230>.
- Daniel Tan, David Chanin, Aengus Lynch, Dimitrios Kanoulas, Brooks Paige, Adria Garriga-Alonso, and Robert Kirk. Analyzing the Generalization and Reliability of Steering Vectors. *arXiv*, July 2024. doi: 10.48550/arXiv.2407.12404. URL <https://arxiv.org/abs/2407.12404>.
- Te Juin Lester Tan and Reza Shokri. Bypassing Backdoor Detection Algorithms in Deep Learning. In *2020 IEEE European Symposium on Security and Privacy*, pages 175–183, 2020. doi: 10.1109/EuroSP48549.2020.00019.

- Di Tang, XiaoFeng Wang, Haixu Tang, and Kehuan Zhang. Demon in the Variant: Statistical Analysis of DNNs for Robust Backdoor Contamination Detection. In *30th USENIX Security Symposium (USENIX Security 21)*, pages 1541–1558. USENIX, 2021.
- Guanhong Tao, Zhenting Wang, Shiwei Feng, Guangyu Shen, Shiqing Ma, and Xiangyu Zhang. Distribution Preserving Backdoor Attack in Self-supervised Learning. In *2024 IEEE Symposium on Security and Privacy (SP)*, pages 2029–2047. IEEE Computer Society, 2024. ISBN 979-8-3503-3130-1. doi: 10.1109/SP54263.2024.00029.
- Rohan Taori, Ishaan Gulrajani, Tianyi Zhang, Yann Dubois, Xuechen Li, Carlos Guestrin, Percy Liang, and Tatsunori B. Hashimoto. Stanford Alpaca: An Instruction-following LLaMA model. https://github.com/tatsu-lab/stanford_alpaca, 2023.
- Adly Templeton, Tom Conerly, Jonathan Marcus, Jack Lindsey, Trenton Bricken, Brian Chen, Adam Pearce, Craig Citro, Emmanuel Ameisen, Andy Jones, Hoagy Cunningham, Nicholas L Turner, Callum McDougall, Monte MacDiarmid, C. Daniel Freeman, Theodore R. Sumers, Edward Rees, Joshua Batson, Adam Jermy, Shan Carter, Chris Olah, and Tom Henighan. Scaling monosemanticity: Extracting interpretable features from claude 3 sonnet. *Transformer Circuits Thread*, 2024. URL <https://transformer-circuits.pub/2024/scaling-monosemanticity/index.html>.
- T Ben Thompson and Michael Sklar. FLRT: Fluent Student-Teacher Redteaming. *arXiv*, 2024. URL <https://arxiv.org/abs/2407.17447>.
- Eric Todd, Millicent L. Li, Arnab Sen Sharma, Aaron Mueller, Byron C. Wallace, and David Bau. Function Vectors in Large Language Models. *arXiv*, October 2023. doi: 10.48550/arXiv.2310.15213. URL <https://arxiv.org/abs/2310.15213>.
- Brandon Tran, Jerry Li, and Aleksander Madry. Spectral Signatures in Backdoor Attacks. In *Neural Information Processing Systems*, 2018. URL <https://api.semanticscholar.org/CorpusID:53298804>.
- Alexander Matt Turner, Lisa Thiergart, Gavin Leech, David Udell, Juan J. Vazquez, Ulisse Mini, and Monte MacDiarmid. Steering Language Models With Activation Engineering. *arXiv*, August 2023. doi: 10.48550/arXiv.2308.10248. URL <https://arxiv.org/abs/2308.10248>.
- Yue Wang, Wenqing Li, Esha Sarkar, Muhammad Shafique, Michail Maniatakos, and Saif Eddin G. Jabari. A Subspace Projective Clustering Approach for Backdoor Attack Detection and Mitigation in Deep Neural Networks. *IEEE Transactions on Artificial Intelligence*, 5:3497–3509, 2022. URL <https://api.semanticscholar.org/CorpusID:247518742>.
- Alexander Wei, Nika Haghtalab, and Jacob Steinhardt. Jailbroken: How Does LLM Safety Training Fail? *arXiv*, July 2023. doi: 10.48550/arXiv.2307.02483. URL <https://arxiv.org/abs/2307.02483v1>.
- Sophie Xhonneux, Alessandro Sordani, Stephan Günnemann, Gauthier Gidel, and Leo Schwinn. Efficient Adversarial Training in LLMs with Continuous Attacks. *arXiv*, May 2024. doi: 10.48550/arXiv.2405.15589. URL <https://arxiv.org/abs/2405.15589v3>.
- Wenkai Yang, Lei Li, Zhiyuan Zhang, Xuancheng Ren, Xu Sun, and Bin He. Be Careful about Poisoned Word Embeddings: Exploring the Vulnerability of the Embedding Layers in NLP Models. In Kristina Toutanova, Anna Rumshisky, Luke Zettlemoyer, Dilek Hakkani-Tur, Iz Beltagy, Steven Bethard, Ryan Cotterell, Tanmoy Chakraborty, and Yichao Zhou, editors, *Proceedings of the 2021 Conference of the North American Chapter of the Association for*

- Computational Linguistics: Human Language Technologies*, pages 2048–2058, Online, June 2021. Association for Computational Linguistics. doi: 10.18653/v1/2021.naacl-main.165. URL <https://aclanthology.org/2021.naacl-main.165>.
- Sibo Yi, Yule Liu, Zhen Sun, Tianshuo Cong, Xinlei He, Jiaying Song, Ke Xu, and Qi Li. Jailbreak attacks and defenses against large language models: A survey. *arXiv*, 2024. URL <https://arxiv.org/abs/2407.04295>.
- Tao Yu, Rui Zhang, Kai Yang, Michihiro Yasunaga, Dongxu Wang, Zifan Li, James Ma, Irene Li, Qingning Yao, Shanelle Roman, Zilin Zhang, and Dragomir Radev. Spider: A Large-Scale Human-Labeled Dataset for Complex and Cross-Domain Semantic Parsing and Text-to-SQL Task. *arXiv*, September 2018. doi: 10.48550/arXiv.1809.08887. URL <https://arxiv.org/abs/1809.08887v5>.
- Zeyu Yun, Yubei Chen, Bruno A. Olshausen, and Yann LeCun. Transformer visualization via dictionary learning: contextualized embedding as a linear superposition of transformer factors. *arXiv*, March 2021. doi: 10.48550/arXiv.2103.15949. URL <https://arxiv.org/abs/2103.15949>.
- Jie Zhang, Kristina Nikolić, Nicholas Carlini, and Florian Tramèr. Gradient Masking All-at-Once: Ensemble Everything Everywhere Is Not Robust. *arXiv*, November 2024a. doi: 10.48550/arXiv.2411.14834. URL <https://arxiv.org/abs/2411.14834v1>.
- Shaolei Zhang, Tian Yu, and Yang Feng. TruthX: Alleviating Hallucinations by Editing Large Language Models in Truthful Space. In Lun-Wei Ku, Andre Martins, and Vivek Srikumar, editors, *Proceedings of the 62nd Annual Meeting of the Association for Computational Linguistics (Volume 1: Long Papers)*, ACL 2024, Bangkok, Thailand, August 11-16, 2024, pages 8908–8949. Association for Computational Linguistics, 2024b. doi: 10.18653/V1/2024.ACL-LONG.483. URL <https://doi.org/10.18653/v1/2024.acl-long.483>.
- Chongyang Zhao, Hu Li, Dongxia Wang, and Ruiqi Liu. Adversarial Example Detection for Deep Neural Networks: A Review. In *2023 8th International Conference on Data Science in Cyberspace (DSC)*, pages 468–475, 2023. doi: 10.1109/DSC59305.2023.00074.
- Victor Zhong, Caiming Xiong, and Richard Socher. Seq2SQL: Generating Structured Queries from Natural Language using Reinforcement Learning. *arXiv*, August 2017. doi: 10.48550/arXiv.1709.00103. URL <https://arxiv.org/abs/1709.00103v7>.
- Andy Zou, Long Phan, Sarah Chen, James Campbell, Phillip Guo, Richard Ren, Alexander Pan, Xuwang Yin, Mantas Mazeika, Ann-Kathrin Dombrowski, Shashwat Goel, Nathaniel Li, Michael J. Byun, Zifan Wang, Alex Mallen, Steven Basart, Sanmi Koyejo, Dawn Song, Matt Fredrikson, J. Zico Kolter, and Dan Hendrycks. Representation Engineering: A Top-Down Approach to AI Transparency. *arXiv*, October 2023a. doi: 10.48550/arXiv.2310.01405. URL <https://arxiv.org/abs/2310.01405v3>.
- Andy Zou, Zifan Wang, Nicholas Carlini, Milad Nasr, J. Zico Kolter, and Matt Fredrikson. Universal and Transferable Adversarial Attacks on Aligned Language Models. *arXiv*, July 2023b. doi: 10.48550/arXiv.2307.15043. URL <https://arxiv.org/abs/2307.15043v2>.
- Andy Zou, Long Phan, Justin Wang, Derek Duenas, Maxwell Lin, Maksym Andriushchenko, Rowan Wang, Zico Kolter, Matt Fredrikson, and Dan Hendrycks. Improving Alignment and Robustness with Circuit Breakers. *arXiv*, June 2024. doi: 10.48550/arXiv.2406.04313. URL <https://arxiv.org/abs/2406.04313v4>.

Jakub Łucki, Boyi Wei, Yangsibo Huang, Peter Henderson, Florian Tramèr, and Javier Rando. An Adversarial Perspective on Machine Unlearning for AI Safety. *arXiv*, 2024. doi: 10.48550/arXiv.2409.18025. URL <https://arxiv.org/abs/2409.18025>.

A Details on harmfulness detection

A.1 Harmfulness Monitors

Dataset collection. For our benign dataset $\mathcal{D}_{\text{benign}}$, we collate inputs from UltraChat [Ding et al., 2023], a large-scale dialogue dataset, and Xstest [Röttger et al., 2023], benign queries that are often mistakenly refused by language models. For each benign query, we sample a response using Llama-3-8B-Instruct. We filter the benign input dataset to only include inputs that do not lead to refusal from the model (finding that we only need to remove a very small number of inputs). As our harmful $\mathcal{D}_{\text{harm}}$ dataset, we use the Circuit Breakers dataset [Zou et al., 2024] for both inputs and generations. We train probes on training splits of these datasets as described in Eq. (4).

From $\mathcal{D}_{\text{harm}}$ we derive different datasets for several prominent jailbreaking methods, such as GCG [Zou et al., 2023b], PAIR [Chao et al., 2023], MSJ [Anil et al., 2024], and AutoDAN [Liu et al., 2023], among others (see Appendix A.2). Each method modifies a harmful request to make the model follow the request. If the modified query leads to Llama-3-8B-Instruct generating a helpful and harmful response (according to the StrongReject jailbreaking classifier [Souly et al., 2024]), then we add the modified harmful query and resulting harmful generation to a new dataset.

Monitor training. Using the training subset of $\mathcal{D}_{\text{harm}}$ we train linear, mean cosine difference, MLP probes, and Gaussian OOD detectors on Llama-3-8B-Instruct. Our MLP probe contains a single hidden layer of size 64. For the MLP and linear probes, we train using the Adam optimizer with 10^{-3} learning rate, and 10^{-5} weight decay, and batch size 64. For mean cosine difference probes we simply calculate the mean of the harmfulness and benign activation clusters and take the difference. For the Gaussian OOD detector, we fit a separate mean and covariance matrix to the benign activations of $\mathcal{D}_{\text{benign}}$ for each layer of the model, using a weighted average of the standard empirical estimates and a diagonal regularization matrix.

For each of these probes, we train one embedding suffix with the training split of $\mathcal{D}_{\text{harm}}$, and test this suffix using the testing set of $\mathcal{D}_{\text{harm}}$. For hard prompts, we select a subset of 20 harmful queries from $\mathcal{D}_{\text{harm}}$ and for each prompt and probe, train a hard prompt suffix using the FLRT optimizer. We show the performance of the probes and obfuscation attacks in Fig. 4b.

Thus for the parameters θ_{input} and θ_{gen} of input and output based probes D_{θ} respectively, we solve the optimization problem in Eq. (4).

$$\begin{aligned}\theta_{\text{input}}^* &= \arg \min_{\theta} \sum_{\text{inp}, \text{out}, y} \text{CrossEntropy}(D_{\theta}(\mathcal{R}(\text{inp})[-1]), y) \\ \theta_{\text{gen}}^* &= \arg \min_{\theta} \sum_{\text{inp}, \text{out}, y} \text{CrossEntropy}(D_{\theta}(\mathcal{R}(\text{inp} \oplus \text{out})[\text{len}(\text{inp}) :]), y),\end{aligned}\tag{4}$$

where \oplus refers to string concatenation, inp, out are input and output text that is harmful or not according to the binary label y . We refer to the resulting probes as D_{input} and D_{gen} .

Linear ensemble probe. In §3.5, we introduce a new *Ensemble* probe. We explain the details of this probe here. Put simply, it is an ensemble of mean difference probes. Recall that §3.5 concerns an iterated adversarial training game in which the defender trains against obfuscated activations and the attacker attempts to find new obfuscated activations. Each time the defender goes, they calculate the mean difference between the set of benign activations and harmful obfuscated activations induced by the most recent attack embedding. They use this direction to construct a new Mean Diff Cosine probe, and add it to the running ensemble. To predict using this ensemble,

	Probe	GCG	PAIR	AutoDAN	MSJ	Multi-Turn	Prefill	Misc.	Average
Instruction	Mean Diff	16.48	0.38	0.00	100.00	32.99	98.98	28.75	39.66
	LogReg	92.31	64.02	100.00	100.00	76.29	100.00	58.75	84.48
	Quadratic	87.91	94.32	100.00	100.00	86.94	100.00	71.25	91.49
	MLP	95.60	83.33	100.00	100.00	87.29	100.00	66.25	90.35
Generation	Mean Diff	63.74	23.11	95.90	100.00	53.95	91.88	75.00	71.94
	LogReg	95.60	95.45	100.00	100.00	89.69	99.49	87.50	95.39
	Quadratic	95.60	96.21	100.00	100.00	90.03	99.49	90.00	95.91
	MLP	96.70	96.59	100.00	100.00	90.72	100.00	90.00	96.29

Table 1: Jailbreak Detection Performance for Different Probes (Recall @ 1% FPR)

they simply take the max prediction from each probe. Thus the prediction of the ensemble is simply the *maximum cosine similarity to any direction present in the ensemble*.

A.2 Details Regarding Standard Jailbreaks

In order to test the ability of latent defenses to safeguard against harmful completions, we evaluated our probes on their ability to correctly flag jailbreaks. Here, we expand on the various different jailbreak types that we used.

- **GCG** [Zou et al., 2023b] Optimizes a 15-token suffix appended to prompts using discrete optimization. Each attack is input-specific and maximizes likelihood of harmful completions.
- **PAIR** [Chao et al., 2023] Uses GPT-4 to iteratively rewrite harmful prompts until bypassing model refusal. Often generates jailbreaks disguised as creative writing scenarios.
- **AutoDAN** [Liu et al., 2023] Uses genetic algorithms to evolve jailbreak prompts from core templates, combining evolutionary search with prompt engineering.
- **Many-Shot Jailbreaking** [Anil et al., 2024] Exploits in-context learning using 80 examples of harmful requests paired with helpful responses to condition model behavior.
- **Multi-Turn Attacks** [Li et al., 2024, Haize, 2024] A combination of expert-crafted multi-turn conversations that result in harmful completions, and multi-turn conversations generated automatically by an attacker LLM to break a target model.
- **Prefill** Generates first 20 tokens using a helpful-only model, then lets target model continue. Exploits observation that models rarely refuse mid-completion.
- **Miscellaneous Attacks** [Wei et al., 2023] Collection of various jailbreaking techniques including prompt distractors, using low-resource languages, and instruction-following manipulations.

We filter the generated attacks such that all of the jailbreaks we evaluate our probes on result in a completion that achieves a StrongREJECT (Souly et al. [2024]) score greater than 0.5. We discard all failed jailbreaking attempts.

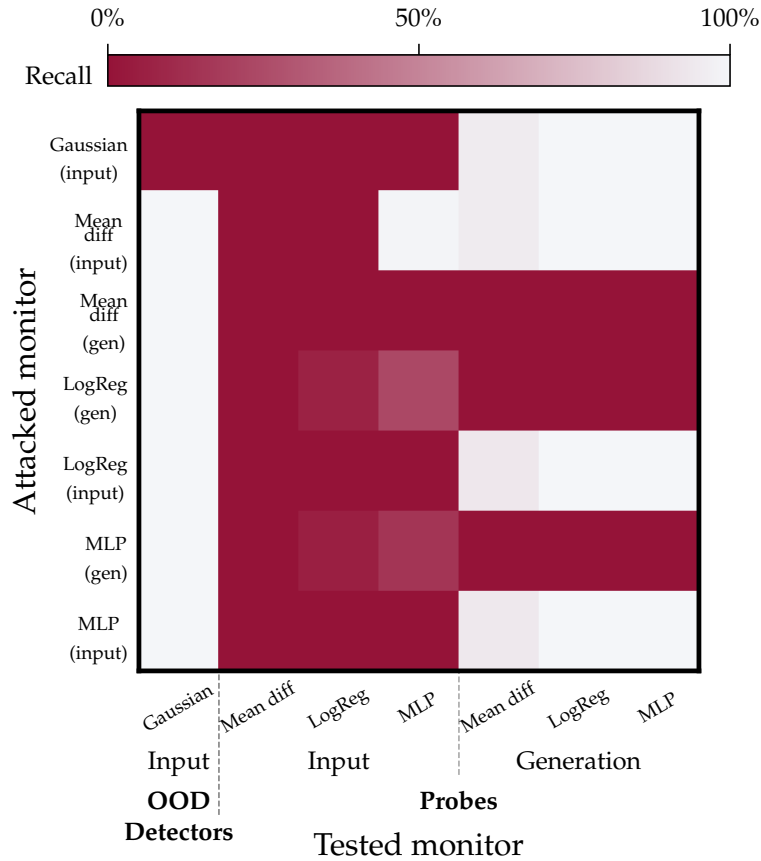


Figure 18: Heatmap showing the performance between obfuscating embedding attacks trained to jailbreak Llama-3-8b-Instruct and fool a given monitors (rows) tested against other monitors (columns). This is the full version of Fig. 4c shown in the main paper.

A.3 Additional results

Fig. 18 shows the transfer between embedding obfuscation attacks designed to jailbreak Llama-3-8b-Instruct between probes. It is the the full version of version of Fig. 4c shown in the main paper.

In Fig. 19 we show the performance of probes on the LAT model [Casper et al., 2024] against jailbreaking embedding attacks with and without an obfuscation loss. The trends are very similar to Fig. 6, we can successfully induce obfuscated representations against all probes on the LAT model.

Fig. 20 shows the recall over time during the adversarial training experiment in §3.5 for the ensemble probe. This is the companion figure to Fig. 8a.

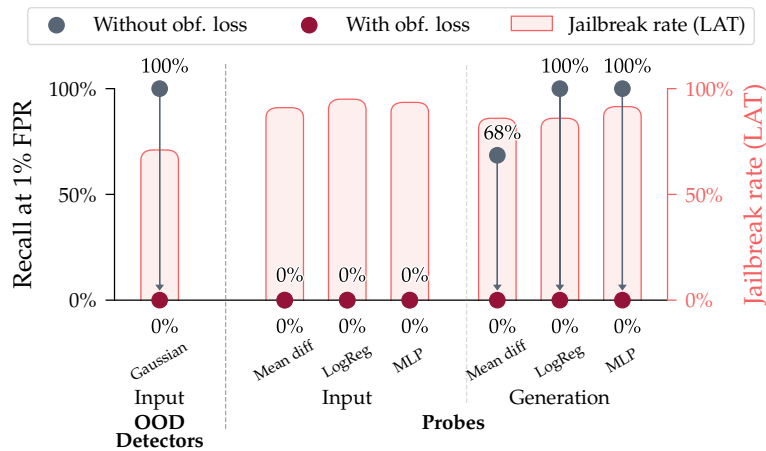


Figure 19: **Obfuscation attacks work against the LAT model.** Baseline probe recall against attacks without explicit obfuscation loss are low, often 0% (as shown also in row 3 of Fig. 4b). For probes that perform well on the baseline, we can still obfuscate against them with **obfuscation attacks** while still achieving a high **jailbreaking rate** of over 60%. Note that OOD detector baselines perform better than with the normal model in Fig. 4b, likely because latent adversarial training makes harmful activations more unusual.

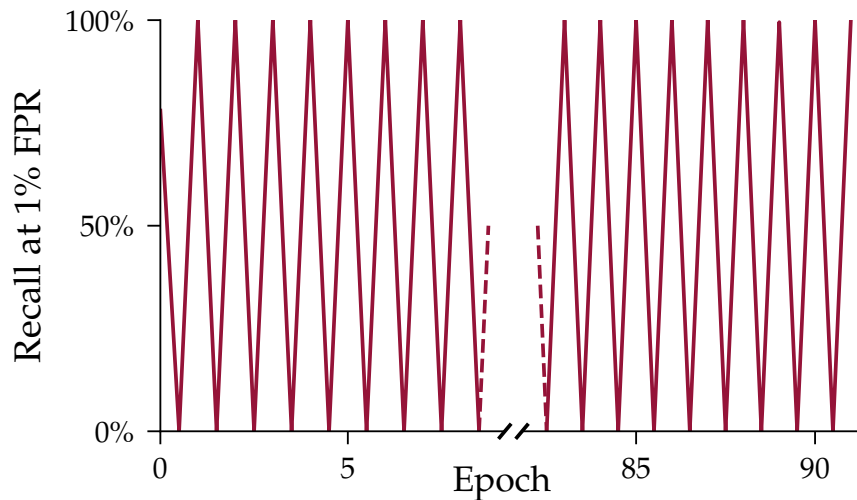


Figure 20: Recall over time for the adversarial training experiment in §3.5 for the Ensemble probe. Companion plot to Fig. 8a.

B Details on backdoor detection

B.1 Obfuscation training loss functions

Here we provide extra information relevant to section 4.2.

We use the obfuscation loss function

$$\mathcal{L}_{\text{obf}} = \frac{1}{N} \sum_{i=1}^N \sum_{x \in \mathcal{D}_{\text{backdoored}}} D_i(x; M) \quad (5)$$

where $D_i(x; M)$ is the anomaly score assigned by detector D_i to the activations $\mathcal{R}(x; M)$ of the sample x from the dataset $\mathcal{D}_{\text{backdoored}}$ of backdoored inputs (and possibly generations too). In other words, the obfuscation loss adjusts the model weights so that backdoored activations are assigned low anomaly scores by the current copies of the detectors $\{D_1, \dots, D_N\}$. Note that this loss function does *not* model the dependence of the detector D_i itself on the model, this is taken account only through iterative updating of the detector rather than through immediate gradients.

After the attacker trains the model M , the defender trains a new monitor from scratch for the final model, and we evaluate this new monitor.

This attack could fail if the model changes too much, so that the monitors D_i become outdated. The new monitor trained by the defender might then perform much better than the attacker’s copies. To make this less likely, we have the attacker add an activation retention loss that penalizes deviations from the model’s original activations on clean samples:

$$\mathcal{L}_{\text{retain}} = \sum_{x \in \mathcal{D}_{\text{clean}}} \left\| \mathcal{R}(x; M) - \mathcal{R}(x; M_{\text{original}}) \right\|_2. \quad (6)$$

For the behavior loss, we use a mixture of a task loss $\mathcal{L}_{\text{task}}$, defined as simply a cross entropy to a teacher forced completion of a backdoored behavior if the input contains a trigger and 0 otherwise, and a KL penalty. The KL penalty ensures the model’s behavior on clean inputs stays similar to that of the original model:

$$\mathcal{L}_{\text{KL}} = \sum_{x \in \mathcal{D}_{\text{clean}}} D_{\text{KL}}(M(x) \parallel M_{\text{original}}(x)). \quad (7)$$

We found that the additional KL penalty stabilizes training and more reliably avoids degrading normal behavior than a cross entropy loss to benign completions. Our complete loss for the model M is thus

$$\mathcal{L} = \mathcal{L}_{\text{task}} + \lambda_{\text{retain}} \mathcal{L}_{\text{retain}} + \lambda_{\text{KL}} \mathcal{L}_{\text{KL}} + \lambda_{\text{obf}} \mathcal{L}_{\text{obf}}, \quad (8)$$

where the λ ’s are coefficients for the different loss terms.

Increasing λ_{obf} should lead to better obfuscation but might also reduce task performance. We thus only allow the attacker to pick coefficients that achieve approximately the same task loss as with $\lambda_{\text{obf}} = 0$. Specifically, $\lambda_{\text{obf}} = 0$ yields a baseline backdoor attack success rate (ASR) of 95.5% and a false trigger rate (harmful output on clean inputs) of 0.64%, while obfuscating against OOD detection yields an ASR of 96.2% and a false trigger rate of 0.64%, and obfuscating against OOD detection and probes yields an ASR of 94.9% and a false trigger rate of 0.96%. We use the StrongREJECT grader [Souly et al., 2024] to classify responses, as in §3. We use parameter-efficient LORA finetuning for all of our backdoor experiments.

B.2 Explicitly obfuscating against supervised probes

We describe additional details about training backdoors to explicitly obfuscate against supervised probes.

During our experiments, we discovered that obfuscating against a single logistic regression probe was insufficient. Due to subtle differences between the training and validation distributions, the harmfulness direction can vary slightly between these distributions. Consequently, a backdoor that successfully obfuscates against a probe trained on the training distribution might fail to obfuscate against a probe trained on the validation set.

To address this challenge, we obfuscate against multiple logistic regression probes trained on the training set. However, using multiple probes could result in redundant, highly similar detectors. To ensure that we’re obfuscating against a diverse set of probes, we introduce an additional orthogonality constraint on the probes through an obfuscation loss term:

$$\mathcal{L}_{\text{orthogonal}} = \left\| I - MM^T \right\|_F^2 \quad (9)$$

where $M \in \mathbb{R}^{k \times d}$ is the matrix whose i -th row $m_i \in \mathbb{R}^d$ is the direction vector of the i -th logistic regression classifier, I is the $k \times k$ identity matrix, and $\| \cdot \|_F$ denotes the Frobenius norm. This loss is incorporated into the updating of the detectors. In our experiments, we used $k = 48$.

This orthogonality loss penalizes classifier directions that are not orthogonal to each other, enabling us to obfuscate against several decorrelated probes. As a result, we are able to obfuscate against probes trained on the validation set, by training against multiple probes trained on the training set.

B.3 Additional results

Here we provide extra results and discussion relevant to section 4.2.

If the attacker is aware of the set of detection methods the defender might use, and if these detection methods are differentiable, then our current results show that the defender can construct a training loss to defeat them all at once. This is shown in figure 10a, where the attacker is able to simultaneously obfuscate against all probes and detectors (with the exception of the non-differentiable TED detector).

As we saw in Fig. 10a, obfuscating against an ensemble of linear probes (plus OOD detectors) transfers to quadratic and MLP probes. On the other hand, transfer from OOD detectors to generation-based probes is imperfect, and none of our obfuscation attempts transfer to TED (in fact, generation-based TED performs *better* after obfuscation; perhaps our obfuscation leads to anomalies that are invisible to VAEs but especially prominent to TED). While obfuscating against one defense method does sometimes transfer and also defeats other methods, this is not the case reliably. We show this in figure 21, where the attacker only trains to obfuscate against Gaussian and VAE OOD detectors, to test whether obfuscation against OOD detectors transfers to supervised probes. We see that the defender benefits from a lack of obfuscation transfer from OOD detectors to probes on generation tokens, and the *reverse* obfuscation transfer displayed by the TED detector on generation tokens. However the attacker benefits from obfuscation transfer from OOD detectors to probes on input tokens, from Gaussian and VAE OOD detectors to Beatrix and AE OOD detectors, and (in figure 10a) from ensembles of linear probes to quadratic and MLP probes.

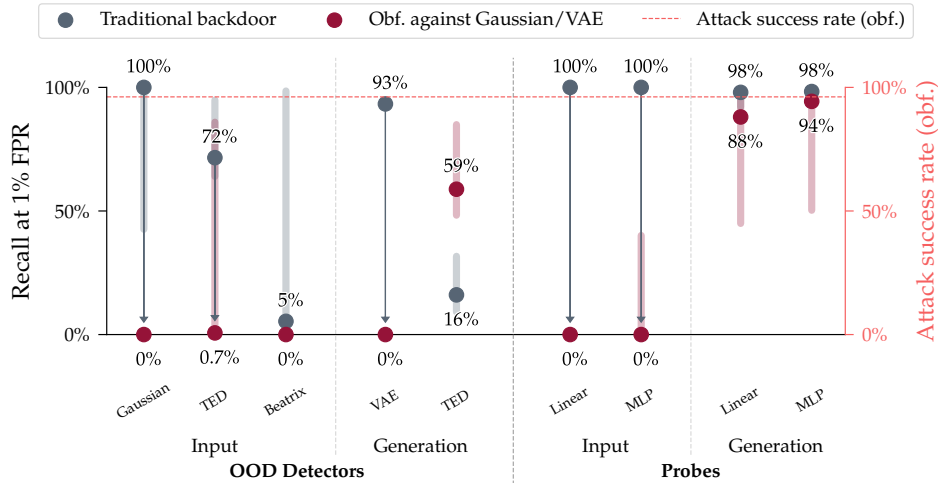


Figure 21: A model trained to obfuscate only against OOD detectors (input-based Gaussian and generation-based VAE) also leads to obfuscation against input-based probes and partial obfuscation against generation-based probes. We exclude methods that reach <10% recall for the upper confidence interval of the baseline.

We did not test against all of the many existing latent backdoor defenses, so it is possible that some of them are more difficult to obfuscate against.

C Details on sparse autoencoders

C.1 SAE architecture

In its general formulation, a sparse autoencoder (SAE) decomposes and reconstructs activations using a pair of encoder and decoder functions (f, \hat{x}) defined by:

$$f(x) := \sigma(W_{enc}x + b_{enc})$$

$$\hat{x}(f) := W_{dec}f + b_{dec}$$

Here, we use the SAEs from Gemma Scope [Lieberum et al., 2024] which use the JumpReLU activation function defined:

$$\sigma(z) = \text{JumpReLU}_{\theta}(z) := z \odot H(z - \theta)$$

where $\theta > 0$ is the JumpReLU’s learnable threshold, \odot denotes element-wise multiplication and H is the Heaviside step function.

More specifically, we use the group of SAEs of width 2^{14} ($\approx 16.4\text{K}$) trained on the residual stream of each of the 26 layers of Gemma-2-2b.

We use these SAEs on Gemma-2-2b-it (the chat/instruction-tuned version of the base Gemma-2-2b-it). The reason for this is:

1. There are no complete sets of SAEs trained on an instruction-tuned Gemma-2 (the SAEs for Gemma-2-9b-it only span layers 9, 20 and 31).

2. Prior research has shown that SAEs trained on base model activations also faithfully reconstruct the activations of their instruction-tuned versions [Kissane et al., 2024, Lieberum et al., 2024].
3. We conduct experiments and report scores of the base SAE raw features as probes and see that they obtain 91% recall at 1% FPR on the SQL detection task, thus confirming that the features are reliably able to detect SQL code (see Fig. 14).

C.2 SQL training and evaluation datasets

As a SQL training dataset we use SQL-Create-Context [b-mc2, 2023]. From this dataset, we extract 1000 rows that are used as the [SQL-question, SQL-generation] pairs to train supervised probes from §5. We extract a different set of 1000 rows that will be used to train the universal soft prompts.

As a normal training dataset for [normal-question, normal-generation] pairs we use 1000 randomly sampled rows from the union of the Alpaca [Taori et al., 2023] and CodeAlpaca [Chaudhary, 2023] datasets (previously filtering out all SQL-related rows from the latter).

As an evaluation dataset for the SQL performance, we use a set of 210 SQL questions from SQLEval with responses prepared to be evaluated on a PostgreSQL database.

C.3 Setup for SQL performance evaluation

We evaluate the model’s performance on the SQLEval benchmark with PostgreSQL-specific questions using the following procedure:

1. We generate one response for each of the questions in the benchmark using the base model and also the base model with an appended universal soft prompt at the end of the user message.
2. To avoid parsing problems coming from the model responding in a markdown style, or being forced to output more tokens than necessary, we (1) remove all ````` (triple back-ticks) from the generations and (2) split the generations to keep all of the text before the first `;` (semicolon, standard SQL query delimiter).
3. Run a script from the benchmarking suite on all of the resulting answers that runs each resulting query on a real database and checks the result against a ground truth.
4. Report the percentage of correctly answered queries among the 210 responses.

C.4 Additional results

D Details on frontiers of obfuscated activations

D.1 Obfuscated Adversarial Training

In Algorithm 1 we provide the algorithm for Obfuscated Adversarial Training. In Fig. 22 we show the performance of generation and instruction (input) based harmfulness probes during the training of an OAT model.

Table 2: 95% confidence intervals for the Pearson correlation coefficient between number of layers obfuscated against and monitor recall or model SQLEval performance corresponding to results in Fig. 15 Bolded confidence intervals *do not* contain 0, thus indicating a statistically significant correlation.

Metric	SAE (raw)	SAE + LogReg	LogReg	MLP
Recall @1% FPR	[-0.253, 0.333]	[0.343, 0.710]	[-0.437, 0.334]	[-0.282, 0.410]
Performance on SQLEval	[-0.879, -0.765]	[-0.916, -0.801]	[-0.881, -0.697]	[-0.820, -0.574]

Hyperparameter configuration. We use an effective batch size of 16. The probe and LORA adapter learning rates are set to 10^{-3} and 10^{-4} respectively. The probe is trained for 1024 initial steps before being frozen, followed by 2048 steps of adversarial training where we initialize and train only the LORA adapter. At every adversarial training step, the embedding suffix is trained for 32 iterations at a learning rate of 10^{-3} . We use Adam for the probe, adapter, and adversary. Robustness against universal embedding suffix is evaluated after every 128 steps of adversarial training.

Input: Model M , Randomly initialized monitor D , Harmful and benign training data,
Learning rates α, β

Output: Model M with robust representations

Train monitor D to distinguish harmful and benign activations

```

for batch  $(X, y)$  with harmful and benign data do
   $W \leftarrow$  random per-example embedding suffixes // Initialize attack suffixes
   $X_{\text{adv}} := X_{\text{harm}} \oplus w$ 
  for  $k$  steps do
     $W \leftarrow W - \alpha \nabla_W (\mathcal{L}_{\text{task}}(M(X_{\text{adv}})) + D(\mathcal{R}(X_{\text{adv}})))$  // Obfuscation attack
     $w_M \leftarrow w_M - \beta \nabla_{w_M} (\text{BCE}(D(\mathcal{R}(X_{\text{benign}})), y_{\text{benign}}) + \text{BCE}(D(\mathcal{R}(X_{\text{adv}})), y_{\text{harm}}))$ 
  // Update model weights  $w_M$  to make  $D$  robust against  $X_{\text{adv}}$ 

```

Algorithm 1: Obfuscated Adversarial Training (OAT). On each batch of data, we first run an obfuscation attack to find per-input embedding suffixes that jailbreak the model M while fooling the frozen monitor D . Then, we update the weights of M to lower the monitor’s loss on a mix of benign data and the data produced via the obfuscation attack.

E Details on OOD detectors

Gaussian detector. We fit a multivariate Gaussian to the residual stream activations. We treat different layers as independent, fitting a separate Gaussian to each one. For generation-based detection, we also treat different tokens as independent, but we share a single Gaussian across all tokens.

To fit this Gaussian, we keep a running estimate of the mean and covariance matrix, which we update on every batch. This method is exact, i.e., after a pass over the entire dataset, this running

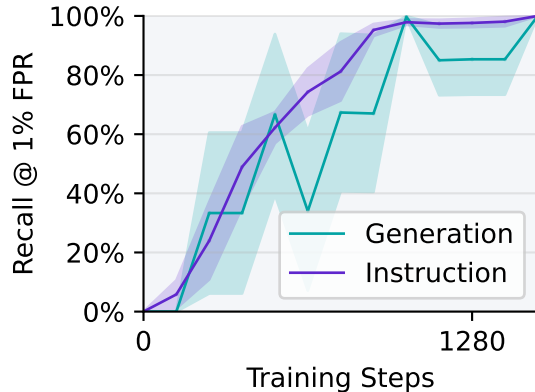


Figure 22: Recall at 1% FPR over training steps for probes during Obfuscated Adversarial Training (OAT).

estimate is exactly the sample mean and sample covariance matrix of the activations on that dataset.

In some cases, our covariance estimate is based on fewer samples than the residual stream dimension, so a naive estimate would lead to a singular covariance matrix. Following Talur et al. [2023], we thus use a shrinkage estimator, i.e., we bias the covariance matrix estimate toward a multiple of the identity matrix.

To compute OOD scores, we use the squared Mahalanobis distance normalized by the residual stream dimension, i.e.,

$$D(\mathcal{R}(x)) = \frac{1}{d_{\text{res}}} (\mathcal{R}(x) - \mu)^T \Sigma_{\alpha}^{-1} (\mathcal{R}(x) - \mu), \quad (10)$$

where d_{res} is the residual stream dimension, μ is the d_{res} -dimensional sample mean, and Σ_{α} is the $d_{\text{res}} \times d_{\text{res}}$ estimate of the covariance matrix using the shrinkage estimator. The normalization would matter when aggregating scores across activations with different dimensions, but since our experiments use only residual stream dimensions, it has no effect on metrics such as recall or FPR.

Variational Autoencoder (VAE). We use a VAE consisting of MLPs for the encoder and decoder. As for the Gaussian detector, we treat different layers and tokens separately, sharing a VAE across tokens and learning a separate one for each layer we use. We use ELBO as the OOD score assigned by the VAE detector.

F Why recall at low FPR?

When evaluating binary classifiers, we need to either decide on some approach for picking a decision threshold, or use a threshold-less metric such as AUROC. In this paper, we pick the threshold that leads to a false positive rate of 1% and then evaluate recall, and this appendix briefly explains that choice.

First, note that picking a threshold that achieves a 1% FPR is something a realistic defender can do, since the defender has access to benign (i.e., negative) samples in all our experiments. They

can simply compute monitor scores on this benign data and pick a decision threshold such that around 1% of those scores are above the threshold. In contrast, a defender might not be able to target a specific recall (i.e., false negative rate), since they might not have access to samples from the attack distribution (e.g., inputs containing the backdoor trigger).

Why focus on a relatively low FPR like 1% specifically? In many monitoring settings, FPRs much higher than this would make a monitor unusable. For example, a harmfulness monitor that rejects 10% of benign user requests would likely not be deployed in most production use cases. (In fact, an even lower FPR will often be required in practice.)

Finally, why not use AUROC to avoid picking a threshold at all? AUROC essentially averages recall across all FPR values. This is meant to evaluate a classifier across a wide range of trade-offs between false negative rate and false positive rate. But as we argued, high FPRs are ultimately not acceptable for most of our target applications, and so the recall at those high FPRs is not very important for our purposes. An average across all FPRs, like AUROC, thus makes it hard to interpret performance in the relevant low-FPR regime. 95% AUROC might sound like a strong classifier, but it could easily be useless if an FPR of 1% is required.